



Interferences caused by the microbial methane cycle during the assessment of abandoned oil and gas wells

Sebastian F. A. Jordan^{1*}, Stefan Schloemer¹, Martin Krüger¹, Tanja Heffner², Marcus A. Horn², Martin Blumenberg^{1*}

¹Federal Institute for Geosciences and Natural Resources (BGR), Hannover, Stilleweg 2, 30655, Germany

²Leibniz Universität Hannover, Institute for Microbiology, Herrenhäuser Str. 2, Hannover, 30419, Germany

Correspondence to: Sebastian F. A. Jordan (Sebastian.Jordan@bgr.de), Martin Blumenberg (Martin.Blumenberg@bgr.de)

Abstract.

In the global effort to reduce anthropogenic methane emissions, the millions of abandoned oil and gas wells are suspected to be prominent but so far often overlooked methane sources. Recent studies highlighted the hundreds of thousand undocumented abandoned wells in North America as sometimes strong methane emitters with up to several tons of methane per year. However, the majority of studies focused on abandoned wells with their surface installations still in place. Only a few studies examined cut and buried wells as their exact location are often unknown. In Germany, approximately 20,000 abandoned wells are described, which are well documented, and the data is publicly available. Here we present a methodological approach to assess methane emissions from such cut and buried abandoned wells. We sampled eight oil wells in a peat rich setting with four wells in a forest, three wells in an active peat extraction site, and one well on a meadow. All three areas have peat deposits underneath. At each site, we sampled a 30 x 30 m grid and a corresponding 20 x 20 m reference grid. Three of the eight well and reference sites showed net methane emissions. The highest emissions with up to $\sim 110 \text{ nmol CH}_4 \text{ m}^{-2} \text{ s}^{-1}$ were observed at one of the reference sites. All three methane-emitting sites were located within the active peat extraction area. Detailed soil gas characterization revealed no methane, ethane, and propane ratio typical for reservoir gas, but instead showed a typical biogenic composition and isotopic signature (mean $\delta^{13}\text{C-CH}_4 - 63\%$). Accordingly, the escaping methane did not originate from the abandoned wells or the connected oil reservoir. In addition, isotopic signatures of methane and carbon dioxide suggest that the peat extraction site's methane was produced by acetoclastic methanogens, whereas methane at the meadow site was from hydrogenotrophic methanogens. However, our genetic analysis showed that both types of methanogens were present at both sites and thus other factors were controlling the prevailing methane production mechanism. Subsequent molecular biological investigations highlighted that aerobic methanotrophs were also important and that they had the highest relative abundance at the peat extraction site. Furthermore, the composition of the methanotrophic community varied across sites and depth. The aerobic methane oxidation rates were highest at the peat extraction site potentially oxidizing a multiple of the emitted methane. Our findings underscore the necessity to combine methane emissions with the characterization of soil gases in comparison with a suitable reference site to survey cut and buried abandoned wells as a solely emission-based surveillance could misinterpret natural occurring emissions.



32

1 Introduction

34 The slow decay of global abandoned oil and gas infrastructure is a rising problem (Bowman et al. 2023, Williams et al. 2021, Riddick et al. 2020) which will intensify in the future during the transition to renewable energy sources. Depending on the
36 country's regulations, abandonment could mean to just close the well head but leave everything in place (Pekney et al. 2020, Williams et al. 2020), decommission the well and leave an open hole in the ground (Pekney et al. 2020, Lebel et al. 2020), or
38 properly fill the well and cut and burry the remains (Schout et al. 2019, Davies et al. 2014). This resulted in varying situations around the world and a general call to action as anthropogenic methane emissions need to be cut (Saunois et al., 2020). Thus,
40 authorities and scientists rush to identify super and mega emitters (Bowman et al 2023) as financial resources for proper well decommission are limited (Agerton et al. 2023). However, this straightforward methodology is only applicable for abandoned
42 wells with visible remains at the surface. In countries with regulations to cut and burry wells (e.g., Germany, the Netherlands, and UK), single measurements at the wells location are insufficient (Schout et al. 2019). Even with correct coordinates,
44 emissions can migrate away from the wells location (Dennis et al 2022, Forde et al. 2022), disperse through the soil and potentially be oxidized by methanotrophic microorganisms on its way to the atmosphere (Forde et al. 2022). In natural methane
46 rich environments, however biogenic methane emissions could be mistaken for a leaking well. An example for such an environment are wetlands and peat rich areas that are associated with a large number of oil and gas wells in Germany.
48 Peat rich areas are former raised/ombrotrophic bogs, rich fens and other types of peat accumulating wetlands. In pristine ecosystems, the vegetation is taking up carbon dioxide from the atmosphere and producing biomass. Plant litter is only partially
50 decomposed due to oxygen limitation in deeper layers. Once oxygen is depleted the microbial degradation of organic carbon is coupled to the reduction of a series of terminal electron acceptors depending on their half-cell potentials (Sikora et al., 2017).
52 Organic carbon degradation is facilitated by a complex network of trophically linked microorganisms (i.e., intermediary ecosystem metabolism) ultimately resulting in methane production when alternative electron acceptors except for carbon
54 dioxide are depleted (Whiticar 2020). Methanogenesis is mainly carried out by three types of anaerobic archaea in more than 30 genera: 1) acetoclastic methanogens converting acetate to methane and carbon dioxide, 2) hydrogenotrophic methanogens,
56 reducing carbon dioxide to methane with hydrogen, and 3) methylotrophic methanogens disproportionating methyl groups to methane and carbon dioxide (Liu and Whitman, 2008). Although most methanogens are hydrogenotrophs, two-thirds of
58 biologically produced methane is derived from acetate (Liu and Whitman, 2008). Is sufficient methane produced, it diffuses towards the surface and it is partially oxidized by anaerobic and aerobic methanotrophs to carbon dioxide along the way.
60 Methanotrophs thereby act as an efficient methane filter and are associated with the regulation of methane fluxes from wetlands. However, these wetlands are still active net carbon sinks, since CO₂ fixation in plant biomass by far exceeds biomass
62 mineralization, and accumulate peat for millenniums (Turetsky et al., 2014; Froelking et al., 2006). Thus, wetlands play a relevant role in the global C cycle as important terrestrial carbon pool (Belyea, 2013).



64 Most raised bogs in Central Europe were, however, drained in the past for agricultural use, forest cultivation, and peat
65 extraction for fuel or horticultural purposes (Pfadenhauer and Klötzli, 1996; Laine et al., 2013). After drainage, most of these
66 wetlands change from net carbon sinks to net carbon sources (Frolking et al., 2006). This is due to the remineralization of once
67 stored organic matter to ultimately carbon dioxide (Abdalla et al., 2016). On the other hand, methane emission decreases
68 drastically as the aerated soil enable aerobic methane oxidation to CO₂ and methanogenesis is restricted to deeper layers (Sundh
69 et al., 1994; Abdalla et al., 2016). Nonetheless, the greenhouse gas balance changes with drainage and differs depending on
70 land use (Abdalla et al., 2016). Methane emissions are thought to stop altogether in peatlands used for forestry or agriculture
71 (Abdalla et al., 2016 and references therein). However, previous studies point towards substantial methane emissions from
72 ditches, which are draining the peats and can even reach the magnitude of emissions from virgin peatlands (Sundh et al., 2000).
73 The extraction of peat results in an accelerated carbon loss and increased greenhouse gas emissions as peat decomposition
74 associated with end use comprises the majority of total emissions (e.g., combustion and use in horticulture machinery for
75 extraction and transportation add additional emissions (Cleary et al., 2005). In this complexity of methane and carbon dioxide
76 related biogeochemical processes, one has to look closely to delicately allocate methane emission to natural or anthropogenic
77 sources.

78 Worldwide only very few countries, i.e., the USA and Canada (Bowman et al., 2023) include emission from abandoned wells
79 in their yearly greenhouse gas inventory. In a BGR project, we aim to fill this knowledge gap for Germany by studying a
80 representative sub-set of wells over the course of five years. Here, we present a first detailed study of eight wells in a complex
81 methane rich setting. In Germany ~ 2700 abandoned wells, which translates to roughly 15% of all abandoned wells (~20,000;
82 NIBIS® Kartenserver 2014) are situated in an organic rich soil (mainly peats) setting (Wittnebel et al., 2023). Such soils are
83 highly likely to produce and emit methane. We used this opportunity to test our methodological approach, a combination of
84 geochemical and microbial techniques, to evaluate methane emissions from cut and buried abandoned wells. Our main focus
85 was on the question of whether we could clearly identify the source of the methane. In addition, the microbiological methods
86 enabled us to quantify the methane oxidation potential of the soil, i.e., the methanotrophic methane filter function, and identify
87 key organisms feeding on the soil methane.

88 2 Methods

2.1 Study site

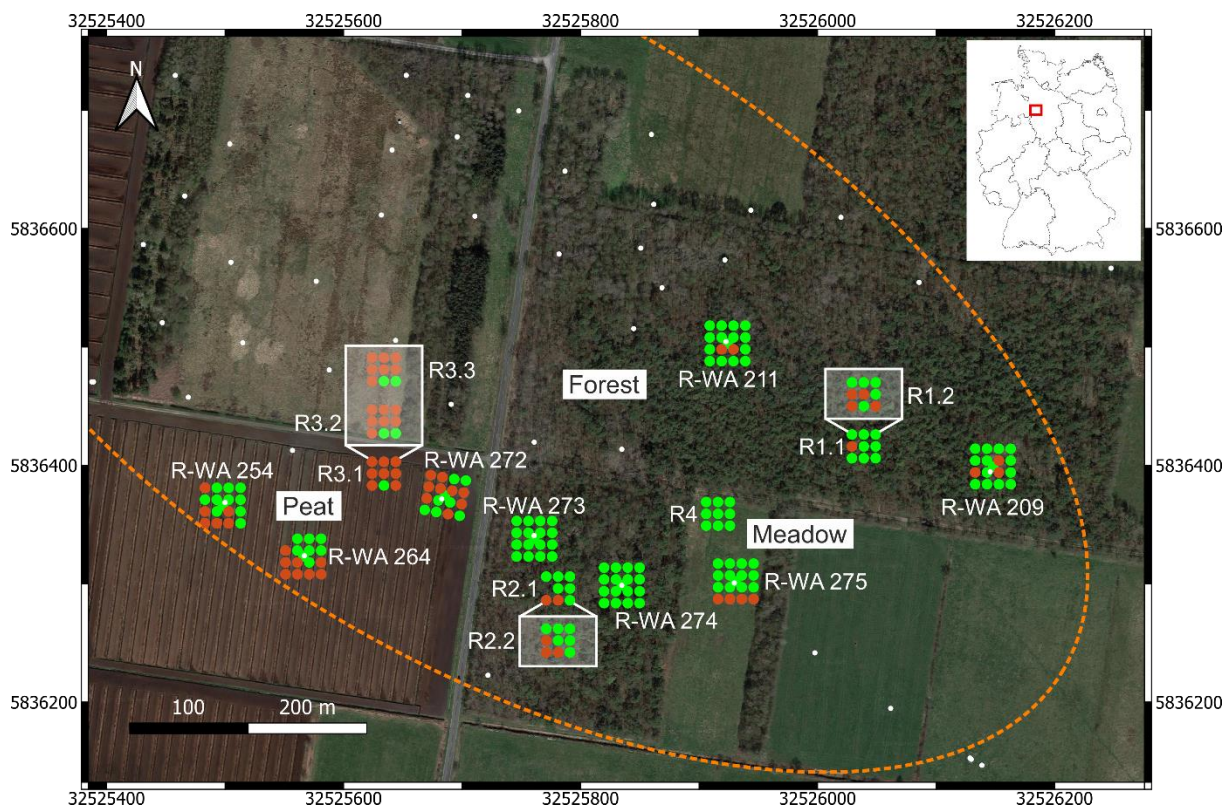
90 The sampling and field measurements were conducted in March and April 2022 near Steimbke (Lower Saxony, Northern
91 Germany), an area with ongoing and historical industrial peat production. Additional samples were taken in April 2023 from
92 the peat extraction site and November 2023 from reference sites. Three oil fields were located around Steimbke. From these
93 three, we focused on field Steimbke-Nord. Data including location, depth, date of drilling, etc. of wells related to this oil field
94 as well as the other ~20,000 wells in Germany (abandoned, producing, and exploration) and data on the oil and gas fields are
publicly available via NIBIS map server (NIBIS® Kartenserver 2014). We used this database to locate about 200 wells in the



96 vicinity of Steimbke-Nord including 159 abandoned production wells. The oil-bearing horizons were located in the Malm and
 98 Dogger (both Jurassic) in 500 and 700 m depth covering an area of about 1.5 km². The wells were drilled between 1942 and
 100 1950 and are typically 570 to 695 m deep. In total 3x10⁸ t oil and 2.9x10⁹ m³ oil associated gas were produced until 1964
 (https://nibis.lbeg.de/cardomap3/?permalink=WeOGYg3, accessed 03.05.2024). We studied and sampled eight abandoned
 102 wells, each with respective reference measurements (Figure 1). These well sites can be grouped into three area types. Three
 out of eight wells (R-WA 254, R-WA 264, R-WA-272) lie in an active peat extraction site (from here on “Peat” sites), four
 104 (R-WA 209, R-WA 211, R-WA 273, R-WA 274) in a woodland area (from here on “Forest”), and one (R-WA 275) on a
 meadow (from here on “Meadow” site). In case of the Forest and Meadow sites, the top soil above the peat layer was sampled,
 106 whereas at the Peat sites the peat was sampled directly. Regarding pH of the Peat site, Welpelo et al. (2024) published a pH of
 ~ 3.5 for a nearby rewetted part of the peat extraction area, about 2.5 km away as well as additional physicochemical
 108 parameters. Residues from the drilling and/or production were only visible in the forest area. Here, cement residues likely from
 the rig cellar or associated infrastructure, sand from the backfill procedure, and small depressions were signs of former activity.
 No residues of the former well itself, like wellheads, old horsehead pumps, or any kind of piping were visible. All sample sites
 are situated in a peat rich area and the majority of sites include about 1.0 m or more raised-bog peat either below the topsoil
 110 (Forest, Meadow) or as bare peat at the Peat site (https://nibis.lbeg.de/cardomap3/?permalink=1baQ8yzX, accessed
 03.05.2024). Peat depth in this area was taken from a geological exploration in 1983. An exemplary soil profile is shown in
 112 Fig. 2d, this profile was drilled near our peat reference site (~ 50 m west). These profiles show a peat thickness of ~1.9 m up
 to 2.6 m for the peat sites with about 1 m and more already extracted since ~2019. For sites R-WA 273, R-WA 274, R-WA
 114 275 the state agency (https://nibis.lbeg.de/cardomap3/?permalink=1uIMU2yt, accessed 03.05.2024) estimated a peat thickness
 of more than 2 m, however, for sites R-WA 211 and R-WA 209 peat was confirmed with more than 30 cm depth but its entire
 116 thickness is unknown.

118 **Table 1:** Overview of surveyed well locations and selected meta data. All wells were used for oil production in the past. *peat is present in
 all areas (Peat = active peat extraction site)

name	short name	north	east	drilling completed	depth (m)	area*
Rodewald-WA-211	R-WA 211	5836503	32525924	26.10.1942	635.5	Forest
Rodewald-WA-209	R-WA 209	5836399	32526148	27.08.1942	570.5	Forest
Rodewald-WA-273	R-WA 273	5836338	32525761	03.08.1950	682.7	Forest
Rodewald-WA-274	R-WA 274	5836299	32525835	04.07.1950	680	Forest
Rodewald-WA-275	R-WA 275	5836302	32525931	21.07.1950	670	Meadow
Rodewald-WA-272	R-WA 272	5836374	32525686	15.06.1950	700	Peat
Rodewald-WA-254	R-WA 254	5836366	32525498	15.12.1948	695	Peat
Rodewald-WA-264	R-WA 264	5836323	32525566	03.06.1950	660	Peat



122 **Figure 1:** Overview of the study site in Steimbke with the well sites and reference site measuring grids each with 17 and 9 measuring points,
 124 respectively. Abandoned wells are depicted in white dots. The rough dimensions of the oilfield Steimbke-Nord are outlined by the yellow
 126 dotted line. Coordinates are stated in UTM-32U (WGS84) with easting and northing planar coordinates in meter. Green indicates negative
 methane emission (methane sink) whereas red indicates positive methane emission (methane source) for each flux measuring point. The
 multiple measurements of reference sites are shown in a white box. The map was created using QGIS (v.3.22.3) and © Google Earth satellite
 images from 2015 as background.

128

2.2 Sampling method and grid

130 We studied well and reference sites for methane emission (positive and negative), soil gas composition and microbial
 community analysis (Figure 2c). The reference sites were placed in a distance of 15–100 m to any well on the same terrain.
 132 The position of the wells was extracted from the NIBIS® MAPSERVER (NIBIS® Kartenserver 2014), and a handheld GPS
 device (Garmin, etrex Vista Hcx) was used to navigate in the field. Due to the burial of abandoned wells in the working area,
 134 our study relied on the coordinates of the wells. Discussion with the LBEG, the local public as well as indications (e.g., color
 changes, remnants of roads/pathways) from recent and historical Google Maps images supported the correctness of the well
 136 positions.

The central measuring point was placed directly above the well. We positioned the other 16 measuring points around the well
 138 pointing north with the help of two measuring tapes and a compass. The distance between these 16 points was 10 m from point



to point aiming at a broad coverage of potential methane emission areas above the buried wells. In total, the well site grid covered an area of 30 x 30 m and 17 measuring points (Figure 2a). Soil gas samples were taken in the central five positions of the well as indicated in Fig. 2a. Soil samples for microbial analyses were usually taken at three positions starting at the center towards one of the corners. In case of high methane emissions, additional soil gas and microbial samples were taken at the respective spots.

The reference grids consisted of nine measuring points covering an area of 20 x 20 m (Figure 2b). Measuring reference grids is necessary to determine and account for potential natural background variations for each abandoned well. Reference grids were typically located in a distance of 50–150 m from the well site and on similar soil conditions and vegetation, and were investigated immediately after the measurement of the well grid. Three soil gas samples were usually taken in a diagonal pattern and the soil sample for microbial analysis in the center of the grid (Figure 2b). To estimate the emission's spatial variability, we sampled a transect through a point with high emission at the Peat reference site. The measuring points along the 12 m transect were 1 m apart.

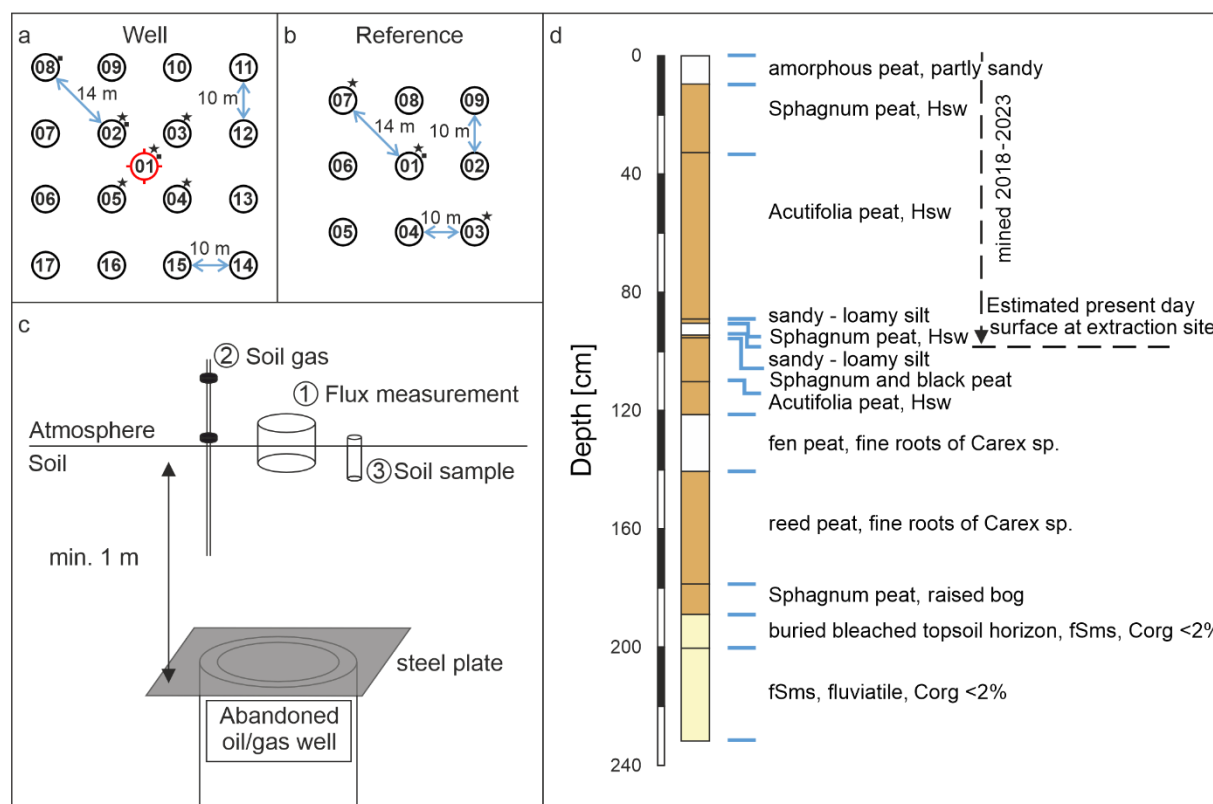


Figure 2: Sampling scheme for emission measurements for well (a) and close-by reference sites (b), both with likely similar biogeochemistry and vegetation, as well as a schematic display of a buried abandoned well (c). Additional soil gas samples (stars) and soil samples for microbial analysis and methane oxidation rates determination (square) were taken at the marked positions. The shift of the symbols towards the upper right was made for graphical reasons. Samples were directly taken on the numbered positions. The well position is marked in red. A simplified profile of a pedological well (# 54315, source LBEG) drilled in 1983 before peat extraction initiated. Coordinates RW: 32525578, HW: 5836405 (EPSG 4647), close (50 m west) to the reference grid in the peat extraction site. fSms: medium sandy fine sand, Hsw: diffuse or in nests enriched with unconsolidated sesquioxides. Link to map <https://nibis.lbeg.de/cardomap3/?permalink=2RfGItuF>.



160 **2.3 Methane and CO₂ emission**

Methane emissions from the soil surface into the atmosphere were measured with an optical feedback – cavity enhanced
162 absorption spectroscopy trace gas analyzer (LI-COR 7810) coupled to a portable hydraulic chamber (LI-COR smart chamber)
following the closed chamber principal. The measurement was conducted as instructed by the manufacturer, which is described
164 in the following: First, defined plastic collars with a diameter of 20.3 cm and height of 12.4 cm (outside diameter 8.4”, height
4.5”) were positioned at each of the measuring points and were pushed few centimeters into the soil to guarantee a complete
166 closure of the smart chamber with the underlying soil profile. Since the exact penetration depths of the collars were needed for
the calculation of fluxes (dead volume of the ring) each insertion depth were measured individually.

168 After both devices, analyzer and chamber, reached operation modus, a startup measurement was conducted to ensure stable
condition of the instrument. Each grid position was sampled in triplicates at least 1 h after placing the respective collar.
170 Therefore, the chamber stayed closed for 120 s to record continuously (1 Hz) the change in methane and carbon dioxide
concentrations in the loop headspace, which was open to the soil surface. Between measurements, the chamber stayed open
172 for 60 s to enable equilibration with atmospheric CH₄ and CO₂ concentrations. Gas fluxes were computed after a dead band
time of 40 s after chamber closing applying a linear regression of the concentration data for each singular measurement,
174 subsequently averaging the triplicate measurements. The standard deviation of the triplicate measurements is tabulated in
supplementary data (Table S2).

176 Additional measurements at each site included soil moisture (SWC) and bulk conductivity measurements (EC) using a Stevens
HydraProbe sensor with 6 cm long measuring rods. The sensor was not particularly calibrated for the organic (peat) rich soils
178 at the study site and used the default “sand” settings for data evaluation. Thus, reported SWC and EC data in Table S2 are only
indicative data. Since the short rods measured the temperature effectively directly below the soil surface with all potential bias
180 to solar radiation, we applied an additional 25 cm long temperature probe (Omega, Type E) to better constrain soil
temperatures.

182

2.4 Soil gas sampling and compositional analysis

184 Gas samples were acquired using soil gas probes. The probes are made of stainless steel with an outer diameter of 6 mm and
inner diameter of 3 mm with a total length of 1.5 m. To prevent the probes from becoming blocked while pushing into the
186 ground, a pin has been attached to the front of the probe. This pin remains in the ground after the desired depth is reached and
the probe was lifted by a few cm. The lances are usually driven into ground with a moveable anvil. However, **at the study site**
188 **with soft unconsolidated sediments** they could easily be pushed into the maximum depth of 1 m. Locations sampled are
indicated in Fig. 2 and wherever methane emission was detected. Due to the shallow ground water table, the probes often had
190 to be lifted close to the surface to be able to sample the gas phase of the vadose zone, thus giving a true indication of the actual



192 water level (sampling depths are listed in Table S1). A septum port is attached to the end of the probe, which allows sampling
with a syringe. Before sampling, the dead volume of the soil gas probe was flushed twice with soil gas immediately after
194 placement with a 20 mL syringe and then rested at least for 1 h to equilibrate. Afterwards 20 mL soil gas was extracted and
stored in crimped vials pre-filled with saturated NaCl as sealing solution. Vials were stored upside down for further gas analysis
in the laboratory.

196 Stored gas samples were analyzed in the lab using a Trace 1310 GC (Thermo Fischer Scientific, USA) equipped with a heated
valve system and column switching. One milliliter of sample was then injected into the sample loops. The individual
198 components were quantified in parallel on three channels.

On channel 1, pre-separation of hydrocarbons (C_1 through C_6) from a 500 μ L sample was performed on a non-polar
200 polysiloxane polymer column (Restek MX-1, 15 m, 0.28 mm ID, film thickness 3 μ m). Molecular weight components $>C_7$
were back-flushed. Full separation was performed on the main 50 m Al_2O_3 capillary column (0.32 mm ID, film thickness 5
202 μ m). Both columns were operated non-isothermally starting at 30 $^{\circ}C$ and ending at 180 $^{\circ}C$. All components were detected on
a Flame Ionization Detector (FID) with helium (He) as carrier gas.

204 On channel 2, the sample was injected via a 500 μ l sample loop. CO_2 was separated from other components by a pre-column
(30 m Hayesep Q, 0.53 mm ID, film thickness 20 μ m) and directly detected after bypassing the Molsieve column on the
206 thermal conductivity detector (TCD). All other components (Ne, H_2 , Ar, O_2 , N_2 , CH_4 , and CO) were chromatographically
separated on the main analytical Molsieve column (80 m 5 Å , 0.53 mm ID, film thickness 50 μ m). Carrier gas on this channel
208 was He.

For better sensitivity for helium and hydrogen, these compounds were analyzed on a channel 3 with argon as carrier gas. The
210 sample loop used had a volume of 125 μ l. CO_2 and higher molecular weight carbon-components were retained and back-
flushed on a packed pre-column (2 m Hayesep Q, mesh 100/120, 1 mm ID). Separation of He, Ne, H_2 , O_2 , and N_2 components
212 was performed on a 5 Å packed molecular sieve column (3 m, mesh 80/100, 1 mm ID) and subsequently detected on a TCD.

214 2.5 Isotopic analysis of methane and carbon dioxide

For samples with concentrations (>200 ppm) carbon isotope signatures of CH_4 ($\delta^{13}C-CH_4$) and CO_2 ($\delta^{13}C-CO_2$) were
216 determined after injecting into a continuous flow GC-IRMS system (Agilent GC coupled to a Thermo Fisher Scientific MAT
253 via a GC-Combustion interface II/III). The different compounds were separated on a 25 m Porapak column and methane
218 was combusted to CO_2 at a temperature of 960 $^{\circ}C$. Low concentration samples (2 – 200 ppm CH_4) were measured applying a
cryo-focusing with liquid nitrogen of methane on a 1 m 1/16 packed column installed in an Agilent 6890 GC likewise coupled
220 to a Thermo Fisher Scientific MAT 253 via a GC-Combustion interface II/III. Deuterium isotope signatures of methane (δ^2H-
 CH_4) were determined by a similar GC-IRMS system (Trace GC and Isolink/ConFlow IV coupled to a MAT 253) if methane
222 concentrations were above 2000 ppm. Methane was reduced to molecular H_2 at a temperature of 1420 $^{\circ}C$. The reproducibility



for $\delta^{13}\text{C}$ is $\pm 0.3\text{‰}$ and for $\delta^2\text{H}-\text{CH}_4 \pm 3\text{‰}$. $^{13}\text{C}/^{12}\text{C}$ and $^2\text{H}/^1\text{H}$ ratios are presented in the standard δ -notation versus the reference
standards Pee Dee Belemnite (VPDB) and Standard Mean Ocean Water (VSMOW), respectively (Coplen, 2011).

2.6 Methane oxidation rates

In the field, shallow soil samples (down to 20 cm) were obtained using a stainless steel push core with an inner Plexiglas liner. Exact coordinates and sampling depth are listed in the supplementary data (Table S4). Deeper samples (40–100 cm) were retrieved with the help of an Edelman auger as a 20 cm composite sample. Samples were kept, transported, and stored at $4-7\text{ °C}$ until further processing. As next step, samples were homogenized and 5 g subsamples were collected and stored at -20 °C for DNA extraction. For determination of potential aerobic methane oxidation rates (MOx) each **sampled** was divided into seven aerobic incubations (100 mL vials), with ~ 10 g homogenized soil sample in each. Three parallels were incubated with 1% methane in the headspace, four without methane with one being autoclaved prior to incubation.

Headspace methane and carbon dioxide concentration were determined regularly with a 610C gas chromatograph (SRI Instruments Europe GmbH, Bad Honnef, Germany) equipped with a flame ionization detector (FID) and a copper methanizer to convert CO_2 to CH_4 . At the end of the incubations, active bottles were subsampled for DNA extraction again (s. section DNA extraction) and then the remaining sample dried at 80 °C to calculate soil water content.

2.7 DNA extraction

DNA was extracted from soil samples (~ 0.5 g) using the FastDNA SPIN kit for soil (MP Biomedicals, Illkirch, France). The extraction followed manufacturer's instructions with modifications as previously described Webster et al. (2003): (1) the addition of 200 μg of poly(adenylic acid) (Roche Diagnostics International Ltd., Rotkreuz, Switzerland) prior to bead beating; (2) two bead beating steps of 45 s at 6.5 m s^{-1} were performed on a FastPrep-24 system (MP Biomedicals); and (3) DNA was eluted in TE-buffer and quantified with the Quantifluor dsDNA chemistry using a Quantus fluorometer (Promega GmbH, Walldorf, Germany).

2.8 Sequencing bacterial and archaeal community via 16S rRNA genes

Following DNA extraction, samples were sequenced by Microsynth AG (Balgach, Switzerland) using MiSeq Illumina technology for microbial community analysis. Both Bacteria and Archaea were sequenced from the same DNA extractions and analyzed separately by targeting the 16S rRNA gene. For bacteria primer pair 515F / 806R (GTG CCA GCM GCC GCG GTAA; GG ACT ACH VGG GTW TCT AAT; Caporaso et al. 2011) and for archaea 340F / ARCH806R (CCC TAY GGG GYG CAS CAG; GGA CTA CVS GGG TAT CTA AT; Takai and Horikoshi 2000; Gantner et al. 2011) were used. Sequences will be deposited in the European Nucleotide Archive (ENA) and the accession number will be published in the final version of the manuscript. Sequences were processed following a bioinformatics pipeline (USEARCH, Edgar 2010; Cutadapt, Martin



254 2011; MOTHUR, Schloss et al. 2009) previously described by Dohrmann and Krüger (2023) to generate zero-radius OTUs
256 (ZOTUs, Edgar 2016). Potentially methanotrophic ZOTUs were identified according to the *pmoA* database taxonomy (Yang
258 et al., 2016) and known methanotrophic genera (Knief, 2015, 2019 and references therein). Relative abundances of a
methanotrophic genus or family were calculated as the share of all methanotrophic genera or families in the respective sample
pool.

260 2.9 Quantification of methane oxidizing bacteria by *pmoA*-gene targeted quantitative PCR

Using a quantitative PCR (qPCR) assays to targeting both, general bacterial 16S rRNA gene and the *pmoA* gene encoding for
262 the β subunit of the particulate methane monooxygenase expressed by methane oxidizing bacteria (MOB), we were able to
determine the methanotrophic abundances.

264 The qPCR targeting the 16S rRNA gene (primer pair 341F/ 805R; forward: 5'-GTGCCAGCMGCCGCGGTAA-3', reverse:
5'-GGACTACHVGGGTWTCTAAT-3') was performed as described previously (Hedrich et al., 2016). The *pmoA* gene
266 targeting qPCR (primer pair 189F/ mb661r; forward: 5'-GGNGACCGGGATTCTGG-3', reverse: 5'-
CAGGMGCAACGTCYTTACC-3'; Costello and Lidstrom 1999) was performed in a CFX Connect real-time PCR system
268 (Bio-Rad, Hercules, CA) in a final volume of 10 μ l, consisting of 5 μ l 2x Luna Universal qPCR Master Mix (New England
BioLabs GmbH, Frankfurt am Main, Germany), 0.7 μ l forward and reverse primers each (10 μ M), 0.5 μ l bovine serum albumin
270 (1 %), 1.1 μ l nuclease-free water and 2 μ l template DNA. The thermal profile consisted of an initial denaturation step at 95 °C
for 5 min, 40 cycles of denaturation at 95 °C for 30 s, annealing at 62 °C for 30 s, elongation at 72 °C for 45 s, and an additional
272 data acquisition step at 79 °C for 8 s, followed by final elongation at 72 °C for 5 min. The template DNA was used in five
times or ten times dilution and spiked with the standard to a concentration of 10⁵ copies per μ l to correct for inhibition.
274 Standards consisted of a dilution series (10¹ – 10⁶ *pmoA* gene copies) of a PCR product flanking the *pmoA* gene of
Methylomonas rhizoryzae GJ1 (Japan Collection of Microorganisms, JCM 33990) amplified with a designed primer pair
276 (forward: 5'-GTACGCATACGCATGAACGC-3', reverse: 5'-GTTTCCCGTGCGTTTGGACTG-3'). The amplicon specificity
was confirmed using a melt curve and agarose gel electrophoresis. Samples that did not show this specificity, i.e., Forest
278 samples, were not considered to calculate *pmoA* abundances.



280 3 Results

3.1 Methane emission

282 To investigate methane emissions related to abandoned onshore wells eight cut und buried wells in the south-eastern part of
the oil field Steimbke-Nord covering an area of $\sim 0.2 \text{ km}^2$ (Figure 1) were targeted. Three wells (R-WA 272, R-WA 254, R-
284 WA 264) are located in the western part of the area where active peat mining is ongoing. One well (R-WA 275), $\sim 350 \text{ m}$ to
the east, is located on a meadow which is temporarily grazed and possibly fertilized with liquid manure. Before the peat
286 extraction in the active area began, the Peat site was also an agricultural meadow that was probably regularly fertilized with
manure. Two of the four wells from the Forest area (dominated by birch trees and pines) are located between the active Peat
288 site and the Meadow (R-WA 273, R-WA 274), the remaining two in a larger forested area $\sim 225 \text{ m}$ to the north and northeast,
respectively.

290 For these eight wells, we established four different reference sites R1 to R4 (Figure 1). The reference site R4 for the abandoned
well on the Meadow was measured once and the two reference sites for the wells in the Forest area (R1 and R2) were each
292 measured twice on consecutive days (Table 2). The single reference site for the three wells in the Peat area (R3) was thus
surveyed three times within one week.

294 In total 64 out of 206 single measurement points showed methane emissions to the atmosphere, however, only the flux of 32
were higher than $1 \text{ nmol CH}_4 \text{ m}^{-2} \text{ s}^{-1}$ and 31 of these were on the Peat site. The absolutely highest flux was $540 \text{ nmol CH}_4 \text{ m}^{-2}$
296 s^{-1} on the Peat site (position 16, site R-WA 264) and the lowest $-4.4 \text{ nmol CH}_4 \text{ m}^{-2} \text{ s}^{-1}$ at the Forest site R-WA 273 position
14 (Table S2).

298 Thirteen out of 17 measuring points of the grid above well R-WA 275 on the Meadow and all corresponding reference
measuring points were a methane sink (up to $-1.2 \text{ nmol CH}_4 \text{ m}^{-2} \text{ s}^{-1}$). Only the four southernmost grid points at the well depict
300 small methane emissions between 0.08 and $0.3 \text{ nmol CH}_4 \text{ m}^{-2} \text{ s}^{-1}$.

All grid points of the wells R-WA 273 and R-WA 274 in the Forest between the Peat site and the Meadow were a methane
302 sink ranging from -4.4 to $-0.03 \text{ nmol CH}_4 \text{ m}^{-2} \text{ s}^{-1}$. Only the reference site (R2.1 and R2.2) showed methane emissions on three
grid points at the southwestern edge consecutively on both measuring day ($< 0.2 \text{ nmol CH}_4 \text{ m}^{-2} \text{ s}^{-1}$, Table S2, Figure 1). Well
304 sites and the reference site in the northern Forest do not reveal a pattern of methane emissions rates. A few grid points of the
well areas (5 out of 34) revealed methane emissions with a singular value exceeding $1 \text{ nmol CH}_4 \text{ m}^{-2} \text{ s}^{-1}$.

306 Results from the well sites and single reference site on the Peat area are more variable. At well R-WA 264 high methane
emission rates have been determined at the southwestern corner including the highest flux rate of $540 \text{ nmol CH}_4 \text{ m}^{-2} \text{ s}^{-1}$. The
308 two nearest grid points to the west still revealed flux rate of $\sim 30 \text{ nmol CH}_4 \text{ m}^{-2} \text{ s}^{-1}$, the highest flux was $540 \text{ nmol CH}_4 \text{ m}^{-2} \text{ s}^{-1}$,
whereas all other points showed slightly positive to negative values. Four well grid points of R-WA 272 revealed high
310 emission rates ranging from 40 to $160 \text{ nmol CH}_4 \text{ m}^{-2} \text{ s}^{-1}$, the highest flux was $540 \text{ nmol CH}_4 \text{ m}^{-2} \text{ s}^{-1}$, these are located at the
northwestern part of the grid close to the reference grid $\sim 50 \text{ m}$ to the northwest. Similar to R-WA 264 all other points showed
312 slightly positive to negative values. Two grid points of well R-WA 254 showed slightly elevated fluxes of $\sim 7 \text{ nmol CH}_4 \text{ m}^{-2}$



314 s^{-1} , the remaining positive emissions being below $0.25 \text{ nmol CH}_4 \text{ m}^{-2} \text{ s}^{-1}$ and all other measurements proving a strong methane sink, up to $-2 \text{ nmol CH}_4 \text{ m}^{-2} \text{ s}^{-1}$.

The reference grid on the Peat site showed always (on three different measuring campaigns) substantial positive methane emissions ranging from 15 to $380 \text{ nmol CH}_4 \text{ m}^{-2} \text{ s}^{-1}$ but only at the northern and middle transect lines. The southern three points always represented a sink or the emissions were lower than $0.2 \text{ nmol CH}_4 \text{ m}^{-2} \text{ s}^{-1}$.

318 As a simple first approximation, we averaged all measuring points of the individual well and reference grids (mean and median, Table 2). However, this should not be directly compared to more sophisticated emission techniques, e.g. long term eddy covariance studies, but rather as a snapshot of our study site for internal comparison of wells/references and different grounds (Forest, Meadow, Peat).

322 Mean and median values that are close to each other are typical for symmetrical distributions with minimal outliers. This holds for the data from the Forest and Meadow for both well and reference site (Table 2, Figure 3a, d). The data from the Peat site show means that are much higher than medians indicating positively skewed data i.e. outliers on the high end (compare histogram Figure 3g). However, as such outliers can control emissions of an area the mean is more suitable. On the other hand, the difference between these two indicates the huge variation in emissions at the Peat site. This is particularly evident at R-WA 264 with one grid point showing $560 \text{ nmol CH}_4 \text{ m}^{-2} \text{ s}^{-1}$ and only two additional points with $30 \text{ nmol CH}_4 \text{ m}^{-2} \text{ s}^{-1}$. All other 14 values are negligible small positive or representing a sink, thus the median of this grid is negative whereas the mean is positive ($38 \text{ nmol CH}_4 \text{ m}^{-2} \text{ s}^{-1}$).

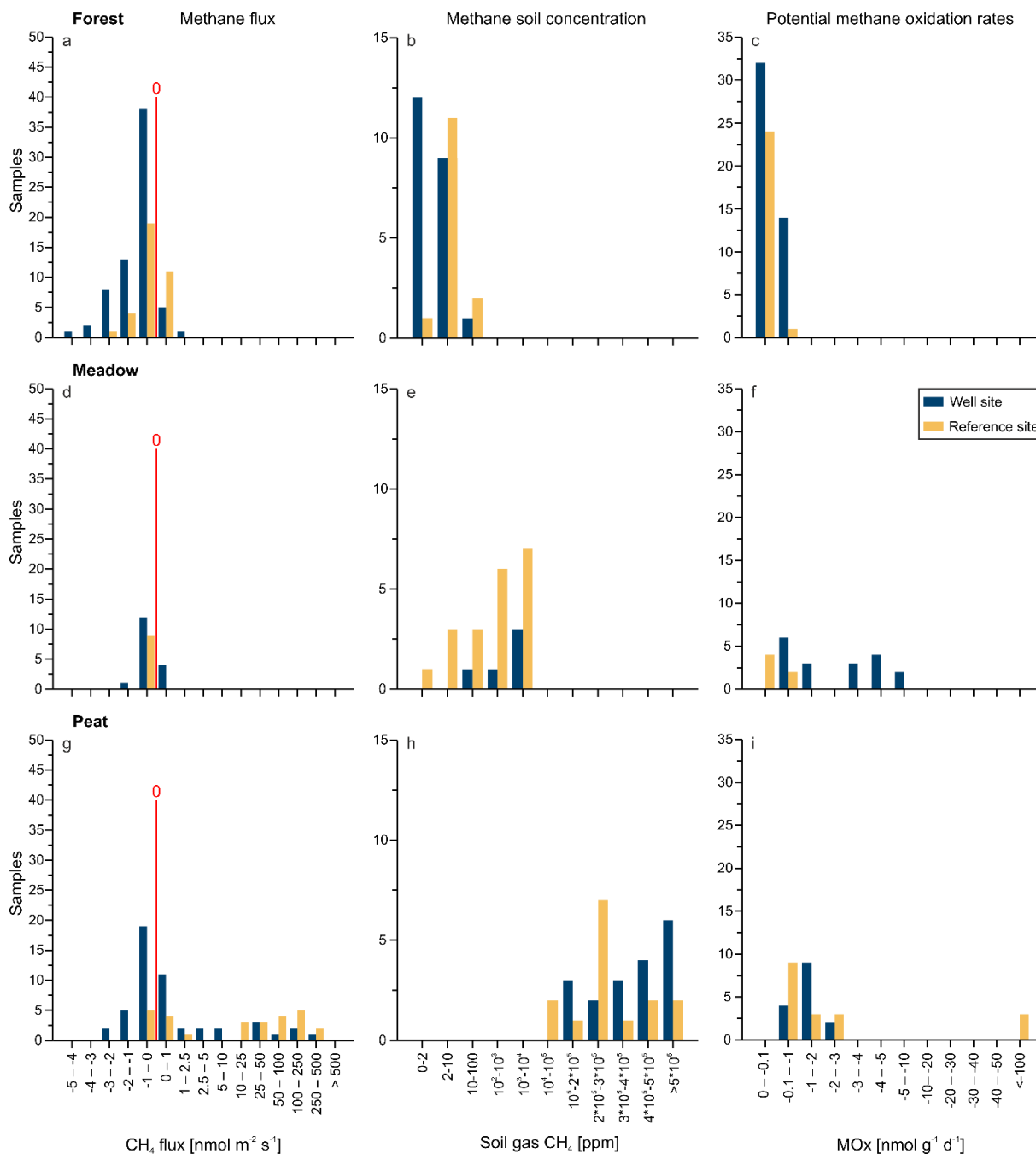
330 Summarizing, all three well sampling grids, for which we observed overall methane emissions based on the mean values of 17 grid points covering an area of 900 m^2 around the well, were located in the Peat area. At wells R-WA 254 and R-WA 264 highly localized methane emissions with high flux rates occur. These singular grid points with high emissions are not spatially correlated with the well location. Moreover, averaged methane emissions (both mean and median) were even consistently higher at the Peat reference site than well sites in the Peat area (Table 1). All four Forest wells were a stronger sink than the corresponding reference sites at the day of measurement. The Forest's acted as a higher methane sink than the Meadow site.

336



Table 2: Summary of the sampled oil well and reference sites.

short name	date	area	CH ₄ flux [nmol m ⁻² s ⁻¹]		mean soil CH ₄ [ppm]	mean δ ¹³ C-CH ₄ [‰]	mean δ ² H-CH ₄ [‰]
			mean	median			
R-WA 211	09.03.2022	Forest	-0.47	-0.13	1.4	-51	
R1.1		Forest	-0.12	-0.09	2.1	-49.6	
R-WA 209	10.03.2022	Forest	-0.35	-0.16	1.6	-56.3	
R1.2		Forest	-0.08	-0.05	2.1	-49.6	
R-WA 273	30.03.2022	Forest	-1.31	-1.22	1.4	-48.3	
R2.1		Forest	-0.76	-0.87	5.2	-56.1	
R-WA 274	31.03.2022	Forest	-1.41	-1.14	20.3	-61	
R2.2		Forest	-0.51	-0.43	6.7	-58	
R-WA 275	21.04.2022	Meadow	-0.2	-0.2	3,695	-85.4	-222.8
R4		Meadow	-0.1	-0.1	4,467	-99.1	-181.8
R-WA 272	20.04.2022	Peat	25.38	0.31	376,918	-58.4	-338
R3.1		Peat	50.07	15.42	181,802	-64.9	-306.9
R-WA 254	27.04.2022	Peat	0.25	-0.08	286,312	-66.1	-332.1
R3.2		Peat	109.03	55.79	369,909	-63.1	-316.3
R-WA 264	28.04.2022	Peat	37.56	-0.05	537,317	-64	-314.1
R3.3		Peat	50.5	20.91	290,555	-65.9	-304.1

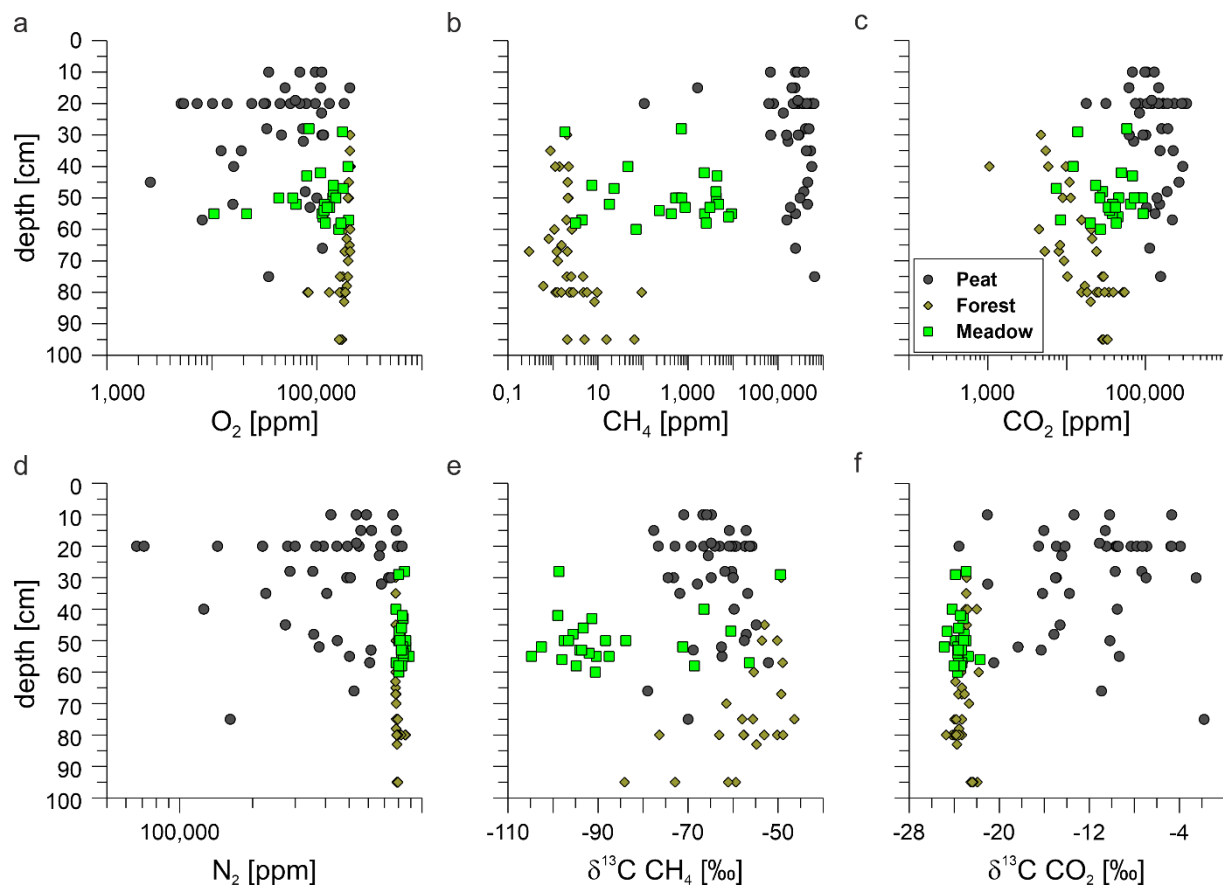


338

340

342

Figure 3: Methane flux (a, d, g), soil gas methane concentration (b, e, h), and potential methane oxidation rates (MOx; c, f, i) depicted as histograms for well (blue) and reference sites (yellow) at the three areas forest (a, b, c), meadow (d, e, f), and peat extraction site (g, h, i). The red line in a, d, g indicates zero flux, sites left of the line acted as net methane sinks and at the right as net methane sources.



344

346

Figure 4: Depth profiles of O_2 (a), CH_4 (b), CO_2 (c), and N_2 (d) soil gas concentrations, as well as $\delta^{13}C$ - CH_4 (e) and $\delta^{13}C$ - CO_2 (f) values for Forest (brown diamonds), Meadow (light green squares) and Peat (dark grey circles) sites. Note the logarithmic scales in a to f. Isotopic composition of methane (d) and carbon dioxide (e) is depicted as difference to the Vienna Pee Dee Belemnite (VPDB) standard.

348



3.2 Soil gas geochemistry

350 Soil gas samples were taken from up to 95 cm depth and analyzed in the laboratory for gas compositions including gaseous
hydrocarbons (C_1 – C_6) as well as carbon and hydrogen isotopic composition if possible. Depths of the soil sampling differed
352 and were determined by the groundwater table. Generally, the sampling depth was closely above the groundwater and is, thus,
an indirect measure of the lower interval of the vadose zone at the time of sampling. The soil methane concentrations between
354 the sampled areas were clearly distinct, with Forest soils showing the lowest methane concentrations compared to Meadow
and Peat (extraction site) soil gases (Figure 3b, e, h and 4b). The majority of methane concentrations at the Forest sites were
356 around or below atmospheric concentrations (Table S1), however, two samples had with ~93 ppm and ~64 ppm elevated
methane concentrations. These Forest sites did not emit substantial amounts of methane (Table 1). The overall mean for
358 samples from Forest soil was ~7.5 ppm methane (Table S1), the median however was ~2.1 ppm, which corresponds to
atmospheric concentrations. Soil methane concentrations in samples from the nearby Meadow site started at ~1.8 ppm and
360 reached up to 9,200 ppm. The respective mean methane concentration was ~1,960 ppm and the median ~710 ppm. Soil gas
samples from the Peat (extraction site) showed both, the highest overall concentration with nearly 65% methane (~645,000
362 ppm) and with ~315,000 ppm (mean) and 282,000 ppm (median) the highest mean and median concentration, respectively.
The general differences in the soil gas composition between the three sampling areas becomes also clear from the plot of all
364 data on O_2 , CH_4 , CO_2 , and N_2 concentrations with depth (Figure 4a–d).

We also analyzed the $\delta^{13}C$ - CO_2 , $\delta^{13}C$ - CH_4 , and δ^2H - CH_4 for most samples (Table S1). Methane concentrations in the Forest
366 soil were, however, too low to determine δ^2H - CH_4 . As for $\delta^{13}C$ - CO_2 , isotopic compositions of Forest and Meadow soil gases
were similar, ranging both between –21.7‰ and –24.9‰, with means of ~–23.3‰ and ~–23.5‰, respectively. Soil gases from
368 the Peat site, on the contrary, were much more ^{13}C -enriched with $\delta^{13}C$ values up to –1.8‰ and a mean of ~–11.6‰. Thus,
while for the Forest and Meadow area $\delta^{13}C$ - CO_2 in the soil gas was relatively uniform and typical for common soil gas,
370 variations at the Peat extraction sites were high, indicative for different controls on soil CO_2 in this area (Figure 4f). The $\delta^{13}C$ -
 CH_4 signatures differed between all three areas with the methane in the Meadow soil being most ^{13}C -depleted with a mean
372 $\delta^{13}C$ value of ~–86.6‰ (–104.8‰ to –49.5‰), in the Forest soil of ~–57.4‰ (–84.1‰ to 46.4‰), and in Peat soil of ~–63.8‰
(–79‰ to –52.2‰; see also Figure 4e). The mean hydrogen isotopic composition of methane differed strongly between the
374 Meadow and Peat soil gases with δ^2H - CH_4 of ~–270‰ and ~–320‰, respectively (Table S1). All isotope data from the
reference and well sites did not show any relevant differences.

376

3.3 Methane oxidation rates

378 Methane oxidation rates were determined to investigate the soils' potential to mitigate methane emissions. In total 27 positions
were sampled in up to two depths, resulting in 46 methane oxidation rates. Following the incubations, the potential oxidation
380 rates were determined per gram dry soil. In addition, we calculated methane oxidation rates for a square meter of wet soil with



20 cm height, which was the maximum aggregated depth for a homogenized soil sample. This way, we got interpolated methane oxidation rates for the sampled soil column that are considered better comparable with measured and published methane fluxes (e.g. calculated per well).

Mean methane oxidation rates per g dry soil (Table 3) were lowest for Forest soils (~ 0.04 nmol g⁻¹ s⁻¹) and highest for soils from the Peat sites (~18.3 nmol g⁻¹ s⁻¹) with intermediate values for Meadow soils (1.4 nmol g⁻¹ s⁻¹). Potential methane oxidation rates per g wet soil sample (single measurements: Table S4) ranged between 2 nmol 0.2 m⁻³ s⁻¹ and ~266 nmol 0.2 m⁻³ s⁻¹ in Forest soils, ~11 nmol 0.2 m⁻³ s⁻¹ and ~8383 nmol 0.2 m⁻³ s⁻¹ at the Meadow, and ~81 nmol 0.2 m⁻³ s⁻¹ and ~150,000 nmol 0.2 m⁻³ s⁻¹ at the industrial Peat site. The respective mean oxidation rates per g wet soil sample (Table 3) for the three studied areas increased from ~47 nmol 0.2 m⁻³ s⁻¹ (Forest) over ~3100 nmol 0.2 m⁻³ s⁻¹ (Meadow) to ~14,100 nmol 0.2 m⁻³ s⁻¹ (Peat extraction site). Mean dry MOx are listed in Table 3.

Table 3: Mean areal methane oxidation rates (MOx) for Forest, Meadow and Peat sites calculated per gram dry soil as well as for dry and wet soil of a volume of 1 m² and 0.2 meter height (= 0.2 m³) as well as mean 16S-RNA gene and *pmoA* abundance per gram dry soil. *pmoA* abundance was calculated as relative to 16S rRNA gene abundances.

	MOx dry [nmol CH ₄ g ⁻¹ s ⁻¹]	MOx dry [nmol CH ₄ 0.2 m ⁻³ s ⁻¹]	MOx wet [nmol CH ₄ 0.2 m ⁻³ s ⁻¹]	16S rRNA gene [10 ⁹ g ⁻¹ dry wt.]	<i>pmoA</i> [10 ⁶ g ⁻¹ dry wt.]	<i>pmoA</i> abundance [%]
Forest	0.04	85	47	13		
Meadow	1.4	2475	3106	16	30	0.19
Peat	18.3	18199	14114	4.6	14	0.30


For a selected experiment on the methane turnover in the Peat area the carbon isotopic fractionation of methane during aerobic methane oxidation was determined in the laboratory (see supplement S2). Using a calculation from (Feisthauer et al., 2011) this resulted in an epsilon (ε) of -31.3‰ (Table S2).

3.4 MOB abundance and identification

We determined MOB abundances by targeting both, the general 16S rRNA gene and *pmoA* gene using qPCR (Table 3). The Peat sites had with ~4.6 x 10⁹ copies g⁻¹ dry weight about three times lower 16S RNA gene copies than the other two sites with 1.3 x 10¹⁰ (Forest) and 1.6 x 10¹⁰ copies g⁻¹ dry weight. The *pmoA* abundances were similar at Meadow and Peat site, with 3.0 x 10⁷ and 1.4 x 10⁷ copies g⁻¹ dry weight, respectively. The relative abundance of the *pmoA* was highest in the Peat (~0.30%) reaching up to 0.89%, followed by the Meadow (0.19%). However, there were huge differences between the samples in each area (Table S5).

We used DNA-based microbial analyses to identify changes in bacterial community over depth and identify potential methanotrophic key player. Bacterial 16S rRNA gene sequencing revealed between ~1.5 x 10⁴ and ~1.35 x 10⁵ sequences per sample with a median of ~8.5 x 10⁴ sequences and a mean library coverage C of >98.5% (data not shown). In total ~22 x 10⁴



410 ZOTUs were determined. A comparison on genus level with published taxa known to contain the *pmo operon* sequences
resulted in up to 151 potential methanotrophic ZOTUs, grouping into 15 methanotrophic genera and 5 families (Table S6).
412 The most abundant putative methanotrophic family in amplicon libraries was *Methylacidiphilaceae*, with 71 uncultured
ZOTUs followed by *Beijerinckiaceae*. The most abundant genera were *Methylocystis* and the uncultured cluster SH765B-TzT-
414 35 from the *Methylomirabilaceae* family (hereafter referred to as SH765B-TzT-35). In the following, we grouped the ZOTUs
belonging to the same genera together in order to simplify the dataset and make changes between the  as better visible.
416 Most reads affiliating with known methanotrophic taxa reads were found at the Peat site, whereas, Forest and Meadow had
about half as much reads. In Forest samples, most of such reads were found in the top layer. On the contrary, they increased
418 with depth for the Meadow site until a depth of 8–13 cm and 15–20 cm at the Peat site and decreased afterwards in both cases
slightly (Table S6). The top layer at Forest and Meadow sites was with regard to methanotrophic taxa dominated by an
420 uncultured *Methylacidiphilaceae* genus, which relative share in reads decreased with depth but was still the most abundant
genus (Figure 5). A member of the genus *Methylocystis*, however, dominated the peat site, its relative abundance first increased
422 to a depth of 20 cm and the abruptly declined at a depth of more than 40 cm. In samples of 40 cm and below SH765B-TzT-35
dominated the methanotrophic community (Figure 5).
424 In addition to bacterial 16S RNA gene sequencing, we used archaeal primer to identify methanogenic key player. Sequencing
resulted into $\sim 9.3 \times 10^3$ and $\sim 1.2 \times 10^5$ reads per sample with a coverage of >99.9% (data not shown). Overall, 798 ZOTU
426 were identified and a comparison with known methanogenic genera revealed 132 potential methanogenic ZOTU (Table S7).
These could be grouped into 11 genera and 9 families (Figure 5). The most abundant genera were *Methanosarcina*, followed
428 by *Methanoregula*, which was almost exclusive present in Peat samples, and third *Methanosaeta*. Together with
Methanobacterium they account for 96% of methanogenic reads over all samples.
430



440 **4 Discussion**

4.1 Evaluation of the methodological approach

442 Abandoned wells in Germany are generally decommissioned and buried (Landesamt für Bergbau, Energie und Geologie
443 (LBEG), 1998). This includes plugging and backfilling of the well, cutting, and removing of the shallow casings, and
444 reconditioning of the area (e.g. for agricultural use). Hence, it is not possible to use the same methods to detect methane from
such wells as for wells with visible surface installations, like partly in the US and Canada (Williams et al. 2021, Lebel et al.
446 2020). As Schout et al. (2019) pointed out, gas leakage of buried wells maybe easily missed by surface measurements alone.
In a study with a strategy comparable to ours, Schout et al. (2019) studied potentially leaking (buried) wells in the Netherlands.
448 While different in some aspects, we, however, also used a tandem approach to detect both methane emissions and methane
concentrations in the soil gas closer to the buried wells. The combination of both methods is necessary, as high soil gas
450 concentrations did not necessarily correspond to high methane emissions at the same spot (Table S1, S2). Probably due to the
high methane oxidation potential of soils in the presence of methanotrophs, as shown previously (Kolb and Horn, 2012; Ho et
452 al., 2019; Guerrero-Cruz et al., 2021). In our case, even measuring points with soil methane concentrations of ~45% of biogenic
methane at 20 cm depth, e.g., site WA-264, position 2, were a methane sink at the surface (Table S1, S2). A similar situation
454 was also observed by Schout et al. (2019), who were unable to detect any methane emissions into the atmosphere above a
leaking borehole that was detectable at a depth of 2 meters below the soil surface.

456 Differences between the areas in our study were more pronounced in soil methane concentrations than in methane emissions.
These emissions ~~on the other hand~~, tended to change from source to sink between two measuring points and, thus, on short
458 distances and eventually over time. We therefore conducted a second sampling campaign at the Peat extraction reference site
with flux measurements only one meter or less apart to better understand variations on a smaller scale than that usually chosen
460 in our study (10 x 10 m). The transect was chosen to pass through a point with high emissions (Figure 6). The resulting methane
fluxes varied more than two orders of magnitude over the distance of less than one meter, whereas CO₂ emissions showed
462 fewer changes and varied in total only by a factor of ~2. This displays the high spatial heterogeneity of the methane emissions
and is in agreement with other soil studies (Davidson et al., 2002; Savage et al., 2014; Ambus and Christensen, 1995; Le Mer
464 and Roger, 2001). To address temporal variation, we revisited reference sites in the Forest and Peat up to three times (Figure
1). The overall flux-pattern at the Peat site changed from one week to another (Figure S4b, d, f) and fluxes at the same spot
466 differed in part greatly (Table 4), whereas fluxes of two consecutive days differed less. However, soil methane concentration
did not vary as much (Table S1). Compared to methane, CO₂ fluxes at the same spots were much more stable and did not show
468 a time dependent variation (Table 4). This temporal data and other data above underline the importance of the use of individual
reference measurements. In addition, we propose with regard to our results that a single measurement is not sufficient to
470 evaluate background emissions properly. Both, spatial and temporal variability could be explained by changes in soil
compaction (Flechard et al., 2007), differences in moisture content (Basiliko et al., 2007), fluctuating macropores (Schwen et



472 al., 2015), differing floras (Jentzsch et al., 2024) and microforms (Welpelo et al., 2024) and fauna (Lubbers et al., 2013).
 474 Furthermore, occurrence of precipitation and air pressure variations between two consecutive measurements could result in
 476 different emission pattern and rates as well (Blagodatsky and Smith, 2012).

Despite the high spatial variation of methane fluxes, we are confident to detect relevant leakage from a well with our strategy
 476 due to (1) the combination of flux and soil gas measurements as well as (2) relying on a 17-point grid instead of single
 measurements. For the grid, we used a distance of 10 m from point to point and ~7 m to the position above the wells at the
 478 center of the grid (Figure 2a). These distances are in between the ones used by Sechman (2022) and Schout et al. (2019) who
 used similar methodical approaches to evaluate the well integrity of buried petroleum and gas wells, respectively.

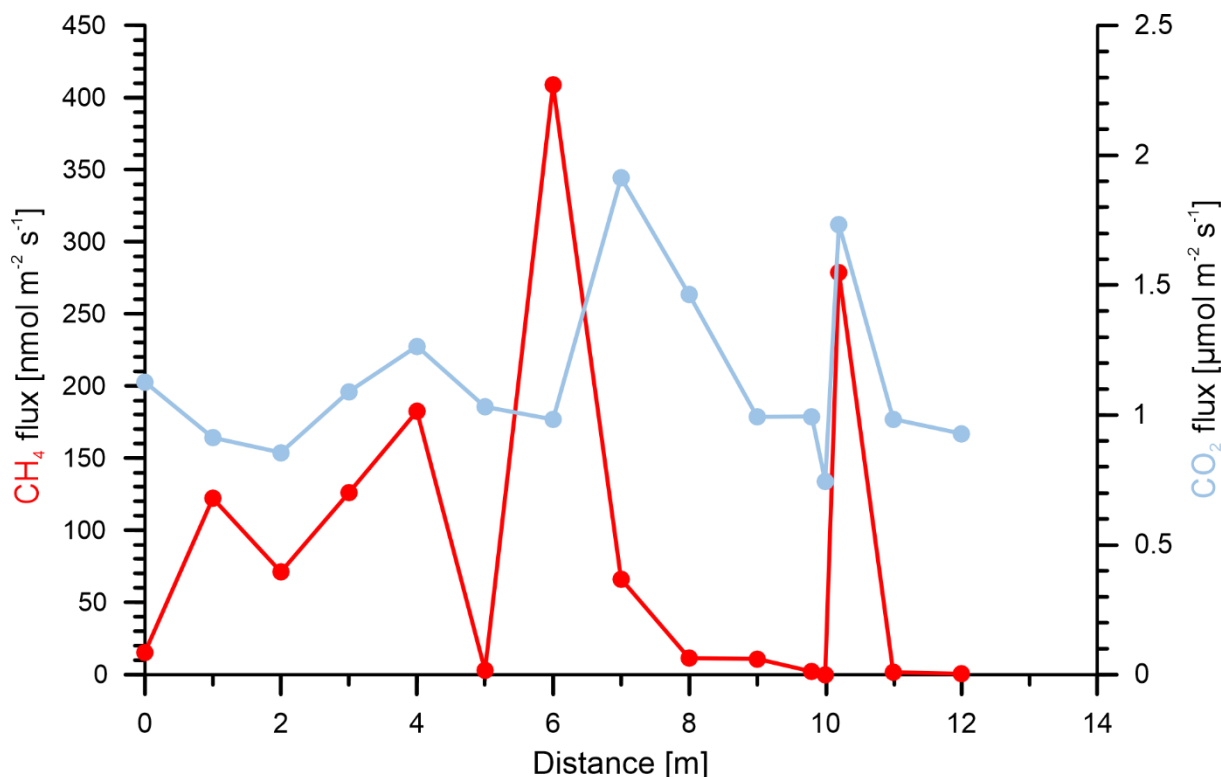
480 Considering the main conclusions from our methodological approach, particularly at Peat sites, high methane concentration in
 addition to methane flux at a well or close-by site does not automatically imply a leaking well, as the methane can also origin
 482 from shallow methanogenesis. Thus, we determined the methane's isotopic composition $\delta^{13}\text{C-CH}_4$ and $\delta^2\text{H-CH}_4$ to distinguish
 between thermogenic (in our case oil-associated) and biogenic methane emissions (Whiticar, 1999; Milkov and Etiope, 2018).
 484 Furthermore, we included measurements of all parameters at reference sites to determine the natural biogeochemical
 background. This approach (see below) helps to get information on whether migration of shallow biogenic methane along the
 486 well takes place (e.g., Vielstädte et al., 2015; 2017) or whether natural biogenic methane sources and processes are responsible
 for methane fluxes.

488

Table 4: Flux measurements at the Peat reference site (ref.) at the exact same coordinates at different time points.

grid-position	CH ₄ [nmol m ⁻² s ⁻¹]			CO ₂ [μmol m ⁻² s ⁻¹]		
	ref. 3.1 20.04.2022	ref. 3.2 27.04.2022	ref. 3.3 28.04.2022	ref. 3.1 20.04.2022	ref. 3.2 27.04.2022	ref. 3.3 28.04.2022
1	273.80	190.43	91.51	3.03	1.66	1.00
2	15.42	381.75	125.38	1.42	2.31	1.70
3	0.21	-0.37	-0.31	1.12	0.76	0.61
4	-0.19	-0.28	-0.26	0.93	0.81	0.54
5	0.02	0.13	0.01	0.44	0.58	0.51
6	31.19	201.39	118.24	1.67	1.87	1.36
7	1.16	55.79	20.91	1.43	2.75	2.53
8	96.14	41.06	15.59	2.72	1.85	1.43
9	32.89	111.38	83.44	1.80	1.38	1.26

490



492

494

Figure 6: Methane (blue) and CO₂ (red) fluxes on a meter scale over a 12 m transect at the peat reference site. The fluxes were measured over the course of 3 h. Data is listed in Table S3.

496

4.2 Assessing contribution of abandoned wells to the methane emissions in the studied areas

498

500

502

504

506

508

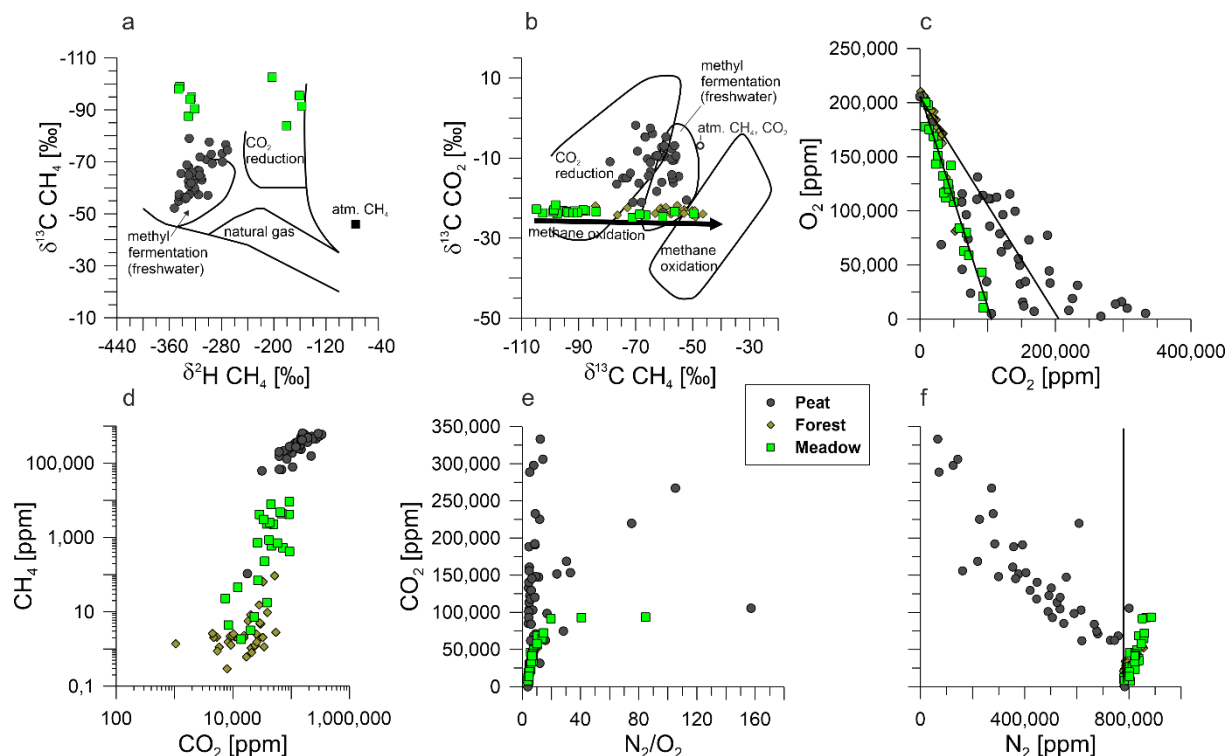
Using our gas geochemical approach, we could identify three well sites and their respective reference measurements with net methane emissions (Table 1), all of which were located at the Peat site. The first indication that the methane emissions were not well-related was that, the reference site emitted more methane than the corresponding well sites (Table 1). All soil gases contained >5% methane with a median of ~35% with no recognizable trend between sites (Table S1). The use of the combination of isotope data on carbon and hydrogen in methane is an established method to identify the methane's source (Whiticar, 1999; Schoell, 1980). Thermogenic gases, which are produced during the maturation of organic material and which occur in natural gases and oil-associated, are characterized by relatively high $\delta^{13}\text{C}$ values ($> \sim -50\%$). In combination with $\delta^2\text{H}$ values of the methane, thermogenic origins (natural gas or oil-associated) can be well recognized in $\delta^{13}\text{C}/\delta^2\text{H}$ diagrams (Figure 7a). None of the isotopically analyzed methane samples from Steimbke showed a signature for thermogenic methane. This excludes the ebullition of relevant amounts of natural gases from the oil reservoir to the atmosphere or upper soils. Further and supporting this conclusion, oil-associated gases and natural gas contain ethane and other higher hydrocarbons, which were also not found in the analyzed gases (Table S1).



Methane concentrations were not sufficient for $\delta^2\text{H}$ analyses in all gas samples, so that the following conclusion does not necessarily hold for low concentrated samples. Our data show that other, distinct biogenic, sources for the methane are likely: methanogenesis using acetate (methyl fermentation; acetoclastic) or CO_2 -reduction (Figure 7b). While our approach cannot exclude well integrity problems in general, our data argue against methane leakage into the upper soil and/or atmosphere from the reservoir for the studied eight wells in the Steimbke-Nord oil field. Furthermore, the high methane emissions at both, well and reference sites, argues against the migration of shallow biogenic methane along the wells (methane concentrations were not higher in the well grid than in the reference grid samples).

Another previously proposed test for well leakage from underground CO_2 -storage sites (Romanak et al., 2017; Romanak et al., 2014) focusses on soil gas composition. The authors argue that oxygen and carbon dioxide concentrations in soil gases, driven by normal microbial respiration, should sum-up to around 21% (Romanak et al., 2012). We observed this in the Forest soil gases (Figure 7c). Single Forest measurements and the majority of the Meadow followed, however, a conversion of 2:1 oxygen to CO_2 , which corresponds to the stoichiometry of aerobic methane oxidation (Romanak et al. 2012; and references therein). The Peat soil gas compositions spread between both processes and conversions. About half of the samples, however, were enriched in CO_2 (up to 33%). According to Romanak et al. (2012), this indicates an addition of CO_2 or oxidation of exogenous CH_4 . The relation of CO_2 to N_2/O_2 is another indication of methane oxidation at the meadow site, however Peat samples indicated excessive CO_2 , too (Figure 7e). Following this narrative, only soil gases at the Peat sites were depleted in N_2 (Figure 7f), which indicates leakage or addition of another deeper gas source displacing the atmospheric nitrogen (Romanak et al., 2012). These findings would point to leakage from the abandoned wells at Steimbke, however as we demonstrated above, isotopic compositions as well as the lack of ethane and propane excludes a thermogenic gas source questioning the possibility to use the model for the interpretation of our study site with a highly active methane cycle. In our view, the drastically increased CO_2 levels in soil gases could be best explained by an extensive microbial degradation of peat via acetate by methanogenesis, which releases methane and CO_2 . This is supported by the Peat's high methane and CO_2 concentrations (Figure 7d). This methane is then oxidized by MOB to CO_2 , which further complicates the soil gas interpretation. In addition, if methane oxidation would be the sole source for the excessive CO_2 , this should be visible in the isotopic signature of methane. However, the in the laboratory determined fractionation factor would result in the more enriched $\delta^{13}\text{C}$ CH_4 and lighter $\delta^{13}\text{C}$ CO_2 . $\delta^{13}\text{C}$ CO_2 was in fact, however, even heavier at the Peat site, which contradicts the interpretation following Romanak et al 2012.

While the soil gas approach by Romanak et al. (2014, 2017) would suggest CO_2 or CH_4 leakage, we were able to disprove this hypothesis in our case. Furthermore, we used this data to look into the apparent differences in methane cycling between the three sites, which will be discussed in the following.



538

540 **Figure 7:** Cross-plots of soil gases, namely isotopic composition of a) methane with regard to stable isotopes of carbon and hydrogen as
 542 well as d) methane and carbon dioxide to characterize the methane's sources, c) methane and carbon dioxide (logarithmic scale), d) oxygen
 544 and carbon dioxide, e) carbon dioxide and the relation of nitrogen and oxygen, f) carbon dioxide and nitrogen for the three sites Peat (grey
 circles), Forest (green diamonds), and Meadow (yellow square). The lines represents in c) left, the consumptions of oxygen via methane
 oxidation and right for normal soil respiration, in f) the atmospheric nitrogen partial pressure. Isotopic composition a+b after Whiticar (1999).
 Comparison of carbon dioxide with oxygen and nitrogen in panels c–f after Romanak et al. (2012).

546 4.3 Natural methane-cycling at the study sites

In natural environments, methane emissions are the result of the interplay between production and consumption, and the biotic
 548 regulation of emissions can occur at the methanogenic and methanotrophic side. Regarding methane production, previous
 studies discussed these possible factors to control methanogenesis (1) availability of acetate due to acetate-oxidizing bacteria
 550 outcompeting CO₂-reducing methanogens (Kotsyurbenko, 2005), (2) phenolic compound concentrations which might limit
 peat degradation in the Forest and Meadow sites (Freeman et al., 2001), (3) and temperature (Brauer et al., 2006). We consider
 552 one or more of these differences also likely to hold for our studied Peat and Meadow areas with the likely different
 predominating methanogenic pathways. Our genetic analysis of the methanogenic community suggests a higher methanogenic
 554 potential at the Peat site (Table S7). *Methanosarcina* and *Methanosaeta* are known acetoclastic methanogens whereas
Methanoregula and *Methanobacterium* are hydrogenotrophic methanogens (Conrad, 2020). At all sites both acetoclastic and
 556 hydrogenotrophic methanogens were present (Figure 5). Soil temperatures were similar at the point of sampling with ~10 °C,



558 which supported the growth of both acetoclastic and hydrogenotrophic methanogens. The isotopic data shown in Fig. 7a, b
underline differences between the sites and suggest that methane was produced via two methanogenic pathways. Namely, the
methane at the Peat site is mostly derived from acetate whereas CO₂ reduction is the main methanogenesis pathway at the
560 Meadow site. This is underlined by the higher mean $\delta^{13}\text{C-CO}_2$ in Peat soil gases (-12‰) compared to soil gases from Meadow
and Forest sites (-23.5‰). One explanation for the site dependent dominant methanogenic pathway could be the differences
562 in peat degradation progression due to the removal of vegetation for peat extraction. The drainage of peatlands is known to
lead to decomposition of peat and results in substantial losses of carbon (Couwenberg, 2011). This may in part explain the
564 higher methane emissions from the active peat extraction site as the drainage of the whole investigate area started already
decades ago. However, only recently (starting 2017/18) the peat extraction started at this site. Thus, we expect that the
566 decomposition of deeper peat layers and the remaining peat intensified after the start of the extraction. Furthermore, about 1
m of peat was extracted from the whole area used for extraction. In addition, this led as we observed to a higher water table,
568 which is one of the main factor for higher methane emission (Abdalla et al., 2016) as it limits oxygen penetration into deeper
layers (Basiliko et al., 2007). For our gas geochemical study and related sampling strategy, however, a respective in-depth
570 understanding of the drivers for the individual methane-formation pathways was beyond the scope of our study and thus we
will focus on the microbial methane filter towards the atmosphere in the following.

572 In the results we point out, that the Forest sites were characterized as a methane sink with soil methane concentrations at
atmospheric levels with one sample at ~ 100 ppm. In addition, Forest soils showed only minor laboratory methane oxidation
574 rates, one explanation for this could be that the present MOB are specialized for low methane concentrations (Bengtson et al.,
2009; Kolb, 2009). The Peat sites on the other hand, showed locally prominent methane fluxes to the atmosphere and methane
576 soil gas concentrations between 1% and 65%. Methane oxidation rates were moderate except for the highest measured rate of
 $150 \mu\text{mol s}^{-1} \text{g}^{-1}$ (wet soil). The Meadow sites acted as net methane sink, soil methane concentrations were mostly above the
578 atmospheric concentration but below 1%, and oxidation rates were moderate. Methane oxidation rates at both Peat and Meadow
sites were, thus, higher than at the Forest site, which coincides with MOB abundance (Table 3). In addition, the higher methane
580 concentrations at the Peat site could enable the growth of low affinity methanotrophs (Christiansen et al., 2014). These
methanotrophs require higher methane concentrations (>100 ppm) but are characterized by higher Michaelis–Menten kinetics
582 (Whiticar 2020, and references therein).

The community analysis revealed a shift from uncultured *Methylacidiphilaceae* at the Forest to members of the *Methylocystis*
584 genus in Peat samples with an additional increase in abundance of Sh765B-TzT-35 (Figure 5). The genus Sh765B-TzT-35
thereby increased with depth and was most abundant in the likely anaerobic layers in the peat at a depth of 40 cm or more.
586 Other members of the *Methylomirabilaceae* family are known to oxidize methane under anaerobic conditions by internal
oxygen production from nitrite reduction to dinitrogen (Ettwig et al., 2010; Versantvoort et al., 2018). Although this was so
588 far not shown for members of Sh765B-TzT-35, a previous study showed their ability to anaerobically oxidize methane
(Nakamura, 2019). Our phylogenic data suggests that members of the *Methylacidiphilaceae* family promote atmospheric
590 methane oxidation whereas *Methylocystis*, *Methylobacter*, and Sh765B-TzT-35 oxidize ascending methane. Kaupper et al.



(2021) who compared pristine and restored peatlands previously observed a similar shift from *Methylacidiphilaceae* to
592 *Methylocystis*. Simplified, one can content that the microbial community at our studied Forest site was similar to that of a
pristine peatland. The active peat extraction site, on the other hand, showed similarity to the restored site in Kaupper et al.
594 (2021). This indicates that starting with peat drainage the methanotrophic community shifts but remains active throughout the
extraction process. However, it takes the microbial community decades to restore pristine-like diversity and complexity
596 (Kaupper et al., 2021). Geochemical and molecular microbial work also underline the differences between all sites. Our
phylogeny analysis were supported by phospholipid fatty acid (PLFA) analyses of selected samples from the Peat site, which
598 indicate that *Methylocystis heyeri*, a Type II (α -Proteobacteria), was likely involved in methane oxidation at these sites (Figure
S1). We also found these PFLA in incubation samples and observed a significant increase after methane addition. Methane
600 oxidation rates were highest in samples with elevated soil methane concentrations (>4000 ppm), which is in concordance with
previous studies (Basiliko et al., 2007; Moore and Dalva, 1997). It was previously shown, that in addition to substrate
602 availability (here methane concentration), the methanotrophic community can be influenced by physico-chemical parameters
and land use (Kaupper et al., 2022) references therein. Kaupper et al. (2022) showed that the environmental parameters, total
604 C and N content, and electrical conductivity, indicative of salinity, affected the active bacterial community. This suggests that
the methanotrophic communities can adapt to different methane regimes and, as speculation, could mitigate a potential leakage
606 over time.

Converting our values for mean methane emissions to enable the comparison with literature data, we observed an emission
608 rate of $\sim 23 \text{ g m}^{-2} \text{ yr}^{-1}$ for the Peat sites. These numbers are in our case without emissions from ditches, which Sundh et al.
(2000) showed can be substantial. An in-depth study on the influence of vegetation on methane emission conducted by Welpelo
610 et al. (2024) at a rewetted peat site about 3 km north-west from our study area, estimated yearly emission between 7.1 and 36.1
 $\text{g m}^{-2} \text{ year}^{-1}$. As our field campaign was conducted in April 2022, and we observed comparable methane emissions to their
612 combination of measurement and modeling for the same season, our yearly estimation seems plausible, although, the Peat's
water table was comparably lower. The emissions at the Peat site's (our study) were about twice (Strack et al., 2016) to more
614 than hundredfold (Wilson et al., 2016) higher than from pristine peat sites and about tenfold from a restored peatland (Strack
et al., 2014). Since carbon dioxide emissions were not elevated, one can assume that the Peat site acted emission wise more
616 like a wetland without vegetation than a drained peatland. In addition, it is possible that the progressed peat extraction provided
a different type and quality of organic precursor substrates than the Forest and Meadow sites as suggested from and observed
618 in other peat sites (Alstad and Whiticar, 2011). Our data suggest that active peat extraction sites do not necessarily emit less
methane than rewetted ones as stated in literature (Welpelo et al., 2024; Bieniada and Strack, 2021; Rankin et al., 2018; Abdalla
620 et al., 2016) and that these areas can be significant methane sources.

Overall, we conclude that there is no connection between the methane emissions detected and the abandoned wells investigated.
622 Furthermore, the factors discussed above suggest that the level of disturbance can be considered as the major driving force for
the here shown methane emissions. Thus, the anthropogenic influences play a key-role for methane formation and emission in
624 such altered ecosystems.



626 5 Conclusion

In the worldwide efforts to mitigate anthropogenic methane emissions, which are a key factor for climate change, a comprehensive approach is needed. One of ~~these~~ sectors is the oil & gas industry and although research targeting abandoned wells developed momentum, financial resources to backfill additional wells are limited (Raimi et al., 2021) and progression advances slowly. Especially orphaned and abandoned wells in the USA and Canada are an active area of research as they are ~~mostly~~ not properly decommissioned and thus prone to leakage. In several studies, high methane emissions (several tons per year) from such wells were observed (i.e., Boutot et al., 2022; Bowman et al., 2023; Hachem & Kang, 2023). Plugged and buried abandoned wells on the other hand were so far poorly studied, and data on location and history of these wells is often limited. ~~In this study, we demonstrate a methodological approach to survey such cut and buried abandoned wells to unravel the methane emissions origin in a complex peat rich setting with a distinctive methane cycle containing several abandoned wells.~~ The approach combined methane flux measurements spanning an area of 30 x 30 m around the well location and a 20 x 20 reference area with the characterization of soil gas samples, and determination of the methane's isotopic composition, respectively. In total, we sampled eight well site, out of which three showed net methane emissions to the atmosphere, all located in an active peat extraction site. However, similar methane abundances at related reference site as well as soil gas and isotopic composition revealed a biogenic origin, thus confirming that the surveilled abandoned wells did not emit methane to the upper soil and atmosphere originating. The methane emission patterns exhibited a substantial spatial variability. Methane concentrations in the soil gas ~~on the other hand~~ were much more homogenous. Subsequent microbial analyses showed substantial methane oxidation capacities at the Peat site. In combination with phylogenetic data, we suggest that established methanotrophic communities act as an efficient aerobic methane filter and may pose as a potential barrier for small leakages. However, further research is necessary to determine their mitigation potential and respective work is ongoing. ~~It remains unclear to what extent natural microbial oxidation capacities for methane could degrade methane in the ground from theoretical leaks in the event of a broken well. However, such processes could be highly relevant for Germany, as 15 % of abandoned wells in Germany are located in areas with highly organic-rich soils such as peat (mostly in Northern Germany). Furthermore, our data showed mean methanotrophy capacities of (wet) peat samples in our lab up to ~14,000 nmol CH₄ 0.2 m⁻³ s⁻¹ (Table 3; = 0.8 g 0.2 m⁻³ h⁻¹). To put this in perspective, methane leakage rates from plugged wells in two regions in Canada ranged between 0.04 to 1 g CH₄ well⁻¹ h⁻¹ (Bowman et al., 2023).~~ ~~Exclusively emission-based approaches, such as the use of emission chambers, survey cars, specialized cameras etc., are not suited for buried wells as they would be susceptible to the misinterpretation of natural methane emissions.~~ For a conclusive surveillance of cut and buried abandoned wells, the here presented multilayered strategy determining methane emissions, soil gas composition and isotopic signatures, ideally together with microbiological techniques in comparison with carefully selected reference sites is necessary.



658 **6 Acknowledgement**

We thank Daniela Zoch, Daniela Graskamp, Thilo Falkenberg, Laurin Rösler, Lukas Heine, Nicole Becker, Alana Zimmer,
660 Georg Scheeder, Dietmar Laszinski, and Christian Seeger for their help in the field and laboratory. Furthermore, we thank
Christian Ostertag-Henning for fruitful scientific discussions and the local peat extraction company for repeated access to the
662 study site. The BGR internal funding through project A-0202019.A and DFG grant HO 6234/1-2 made this study possible.

664 **7 Data availability**

Measured and derived data supporting the findings of this study are available in the supplementary data sheet.

666

8 Author contributions

668 M.B., S.S., S.F.A.J., and M.K. conceived and designed the experiments. S.F.A.J., S.S., M.B., M.K. conducted the fieldwork
and performed the experiments. S.F.A.J. and T.H. performed qPCR and processed the data. Main data interpretation was
670 performed by S.F.A.J. in cooperation with the co-authors. S.F.A.J. wrote the main manuscript text with input from M.B., S.S.,
M.K., T.H., M.A.H. All authors read and approved the final version of the manuscript.

672

9 Competing interests

674 The authors declare no competing interests.



676 7 References

- 678 Abdalla, M., Hastings, A., Truu, J., Espenberg, M., Mander, U., and Smith, P.: Emissions of methane from
northern peatlands: a review of management impacts and implications for future management options, *Ecol*
Evol, 6, 7080-7102, <https://doi.org/10.1002/ece3.2469>, 2016.
- 680 Alstad, K. P. and Whiticar, M. J.: Carbon and hydrogen isotope ratio characterization of methane dynamics for
Fluxnet Peatland Ecosystems, *Org Geochem*, 42, 548-558, <https://doi.org/10.1016/j.orggeochem.2011.03.004>,
682 2011.
- Ambus, P. and Christensen, S.: Spatial and Seasonal Nitrous Oxide and Methane Fluxes in Danish Forest-,
684 Grassland-, and Agroecosystems, *J Environ Qual*, 24, 993-1001,
<https://doi.org/10.2134/jeq1995.00472425002400050031x>, 1995.
- 686 Basiliko, N., Blodau, C., Roehm, C., Bengtson, P., and Moore, T. R.: Regulation of Decomposition and Methane
Dynamics across Natural, Commercially Mined, and Restored Northern Peatlands, *Ecosystems*, 10, 1148-
688 1165, <https://doi.org/10.1007/s10021-007-9083-2>, 2007.
- Belyea, L. R.: Nonlinear Dynamics of Peatlands and Potential Feedbacks on the Climate System, in: *Carbon*
690 *Cycling in Northern Peatlands*, *Geoph Mono*, 5-18, <https://doi.org/10.1029/2008gm000829>, 2013.
- Bengtson, P., Basiliko, N., Dumont, M. G., Hills, M., Murrell, J. C., Roy, R., and Grayston, S. J.: Links between
692 methanotroph community composition and CH₄ oxidation in a pine forest soil, *FEMS Microbiol Ecol*, 70,
356-366, <https://doi.org/10.1111/j.1574-6941.2009.00751.x>, 2009.
- 694 Bieniada, A. and Strack, M.: Steady and ebullitive methane fluxes from active, restored and unrestored
horticultural peatlands, *Ecol Eng*, 169, <https://doi.org/10.1016/j.ecoleng.2021.106324>, 2021.
- 696 Blagodatsky, S. and Smith, P.: Soil physics meets soil biology: Towards better mechanistic prediction of
greenhouse gas emissions from soil, *Soil Biol Biochem*, 47, 78-92,
698 <https://doi.org/10.1016/j.soilbio.2011.12.015>, 2012.
- Bowman, L. V., El Hachem, K., and Kang, M.: Methane Emissions from Abandoned Oil and Gas Wells in
700 Alberta and Saskatchewan, Canada: The Role of Surface Casing Vent Flows, *Environ Sci Technol*,
<https://doi.org/10.1021/acs.est.3c06946>, 2023.
- 702 Brauer, S. L., Cadillo-Quiroz, H., Yashiro, E., Yavitt, J. B., and Zinder, S. H.: Isolation of a novel acidiphilic
methanogen from an acidic peat bog, *Nature*, 442, 192-194, <https://doi.org/10.1038/nature04810>, 2006.
- 704 Caporaso, J. G., Lauber, C. L., Walters, W. A., Berg-Lyons, D., Lozupone, C. A., Turnbaugh, P. J., Fierer, N.,
and Knight, R.: Global patterns of 16S rRNA diversity at a depth of millions of sequences per sample, *Proc*
706 *Natl Acad Sci U S A*, 108 Suppl 1, 4516-4522, <https://doi.org/10.1073/pnas.1000080107>, 2011.
- Christiansen, J. R., Romero, A. J. B., Jørgensen, N. O. G., Glaring, M. A., Jørgensen, C. J., Berg, L. K., and
708 Elberling, B.: Methane fluxes and the functional groups of methanotrophs and methanogens in a young Arctic
landscape on Disko Island, West Greenland, *Biogeochemistry*, 122, 15-33, [https://doi.org/10.1007/s10533-
710 014-0026-7](https://doi.org/10.1007/s10533-014-0026-7), 2014.
- Cleary, J., Roulet, N. T., and Moore, T. R.: Greenhouse gas emissions from Canadian peat extraction, 1990-2000:
712 a life-cycle analysis, *Ambio*, 34, 456-461, <https://doi.org/10.1579/0044-7447-34.6.456>, 2005.
- Conrad, R.: Importance of hydrogenotrophic, acetoclastic and methylotrophic methanogenesis for methane
714 production in terrestrial, aquatic and other anoxic environments: A mini review, *Pedosphere*, 30, 25-39,
[https://doi.org/10.1016/s1002-0160\(18\)60052-9](https://doi.org/10.1016/s1002-0160(18)60052-9), 2020.
- 716 Costello, A. M. and Lidstrom, M. E.: Molecular characterization of functional and phylogenetic genes from
natural populations of methanotrophs in lake sediments, *Appl Environ Microbiol*, 65, 5066-5074,
718 <https://doi.org/10.1128/AEM.65.11.5066-5074.1999>, 1999.



- Couwenberg, J.: Greenhouse gas emissions from managed peat soils: is the IPCC reporting guidance realistic?,
720 Mires Peat, 8, 2011.
- Davidson, E. A., Savage, K., Verchot, L. V., and Navarro, R.: Minimizing artifacts and biases in chamber-based
722 measurements of soil respiration, *Agr Forest Meteorol*, 113, 21-37, [https://doi.org/10.1016/s0168-1923\(02\)00100-4](https://doi.org/10.1016/s0168-1923(02)00100-4), 2002.
- 724 Dohrmann, A. B. and Krüger, M.: Microbial H₂ Consumption by a Formation Fluid from a Natural Gas Field at
High-Pressure Conditions Relevant for Underground H₂ Storage, *Environ Sci Technol*, 57, 1092-1102,
726 <https://doi.org/10.1021/acs.est.2c07303>, 2023.
- Edgar, R. C.: Search and clustering orders of magnitude faster than BLAST, *Bioinformatics*, 26, 2460-2461,
728 <https://doi.org/10.1093/bioinformatics/btq461>, 2010.
- Edgar, R. C.: UNOISE2: improved error-correction for Illumina 16S and ITS amplicon sequencing., *bioRxiv*
730 [preprint], <https://doi.org/10.1101/081257>, 2016.
- Ettwig, K. F., Butler, M. K., Le Paslier, D., Pelletier, E., Mangenot, S., Kuypers, M. M., Schreiber, F., Dutilh, B.
732 E., Zedelius, J., de Beer, D., Gloerich, J., Wessels, H. J., van Alen, T., Luesken, F., Wu, M. L., van de Pas-
Schoonen, K. T., Op den Camp, H. J., Janssen-Megens, E. M., Francoijs, K. J., Stunnenberg, H.,
734 Weissenbach, J., Jetten, M. S., and Strous, M.: Nitrite-driven anaerobic methane oxidation by oxygenic
bacteria, *Nature*, 464, 543-548, <https://doi.org/10.1038/nature08883>, 2010.
- 736 Feisthauer, S., Vogt, C., Modrzyński, J., Szlenkier, M., Krüger, M., Siebert, M., and Richnow, H.-H.: Different
types of methane monooxygenases produce similar carbon and hydrogen isotope fractionation patterns during
738 methane oxidation, *Geochim Cosmochim Acta*, 75, 1173-1184, <https://doi.org/10.1016/j.gca.2010.12.006>, 2011.
- Flechar, C. R., Ambus, P., Skiba, U., Rees, R. M., Hensen, A., van Amstel, A., Dasselaar, A. v. d. P.-v.,
740 Soussana, J. F., Jones, M., Clifton-Brown, J., Raschi, A., Horvath, L., Neftel, A., Jocher, M., Ammann, C.,
Leifeld, J., Fuhrer, J., Calanca, P., Thalman, E., Pilegaard, K., Di Marco, C., Campbell, C., Nemitz, E.,
742 Hargreaves, K. J., Levy, P. E., Ball, B. C., Jones, S. K., van de Bulk, W. C. M., Groot, T., Blom, M.,
Domingues, R., Kasper, G., Allard, V., Ceschia, E., Cellier, P., Laville, P., Henault, C., Bizouard, F., Abdalla,
744 M., Williams, M., Baronti, S., Berretti, F., and Grosz, B.: Effects of climate and management intensity on
nitrous oxide emissions in grassland systems across Europe, *Agric Ecosyst Environ*, 121, 135-152,
746 <https://doi.org/10.1016/j.agee.2006.12.024>, 2007.
- Freeman, C., Ostle, N., and Kang, H.: An enzymic 'latch' on a global carbon store, *Nature*, 409, 149,
748 <https://doi.org/10.1038/35051650>, 2001.
- Frolking, S., Roulet, N., and Fuglestedt, J.: How northern peatlands influence the Earth's radiative budget:
750 Sustained methane emission versus sustained carbon sequestration, *J Geophys Res Biogeosci*, 111,
<https://doi.org/10.1029/2005jg000091>, 2006.
- 752 Gantner, S., Andersson, A. F., Alonso-Saez, L., and Bertilsson, S.: Novel primers for 16S rRNA-based archaeal
community analyses in environmental samples, *J Microbiol Meth*, 84, 12-18,
754 <https://doi.org/10.1016/j.mimet.2010.10.001>, 2011.
- Guerrero-Cruz, S., Vaksmaa, A., Horn, M. A., Niemann, H., Pijuan, M., and Ho, A.: Methanotrophs: Discoveries,
756 Environmental Relevance, and a Perspective on Current and Future Applications, *Front Microbiol*, 12,
678057, <https://doi.org/10.3389/fmicb.2021.678057>, 2021.
- 758 Hedrich, S., Guezennec, A. G., Charron, M., Schippers, A., and Joulain, C.: Quantitative Monitoring of Microbial
Species during Bioleaching of a Copper Concentrate, *Front Microbiol*, 7, 2044,
760 <https://doi.org/10.3389/fmicb.2016.02044>, 2016.
- Ho, A., Kwon, M., Horn, M. A., and Yoon, S.: Environmental Applications of Methanotrophs, in:
762 Methanotrophs, *Micro Mono*, 231-255, https://doi.org/10.1007/978-3-030-23261-0_8, 2019.
- Jentsch, K., Männistö, E., Marushchak, M. E., Korrensalo, A., van Delden, L., Tuittila, E.-S., Knoblauch, C.,
764 and Treat, C. C.: Seasonal controls on methane flux components in a boreal peatland - combining plant



- 766 removal and stable isotope analyses, EGU sphere [preprint], <https://doi.org/10.5194/egusphere-2023-3098>,
2024.
- 768 Kartenserver, N.: Oil & Gas fields - Landesamt für Bergbau, Energie und Geologie (LBEG), Hannover. [dataset],
2014a.
- 770 Kartenserver, N.: Network Hydrocarbon-Geology (KW-Verbund). - Landesamt für Bergbau, Energie und
Geologie (LBEG), Hannover. [dataset], 2014b.
- 772 Kaupper, T., Mendes, L. W., Harnisz, M., Krause, S. M. B., Horn, M. A., and Ho, A.: Recovery in
methanotrophic activity does not reflect on the methane-driven interaction network after peat mining, Appl
Environ Microbiol, 87, <https://doi.org/10.1128/AEM.02355-20>, 2021.
- 774 Kaupper, T., Mendes, L. W., Poehlein, A., Frohloff, D., Rohrbach, S., Horn, M. A., and Ho, A.: The methane-
driven interaction network in terrestrial methane hotspots, Environ Microbiome, 17, 15,
776 <https://doi.org/10.1186/s40793-022-00409-1>, 2022.
- 778 Knief, C.: Diversity and Habitat Preferences of Cultivated and Uncultivated Aerobic Methanotrophic Bacteria
Evaluated Based on *pmoA* as Molecular Marker, Front Microbiol, 6, 1346,
<https://doi.org/10.3389/fmicb.2015.01346>, 2015.
- 780 Knief, C.: Diversity of Methane Cycling Microorganisms in Soils and Their Relation to Oxygen, Curr Issues Mol
Biol, 33, 23-56, <https://doi.org/10.21775/cimb.033.023>, 2019.
- 782 Kolb, S.: The quest for atmospheric methane oxidizers in forest soils, Environ Microbiol Rep, 1, 336-346,
<https://doi.org/10.1111/j.1758-2229.2009.00047.x>, 2009.
- 784 Kolb, S. and Horn, M. A.: Microbial CH₄ and N₂O Consumption in Acidic Wetlands, Front Microbiol, 3, 78,
<https://doi.org/10.3389/fmicb.2012.00078>, 2012.
- 786 Kotsyurbenko, O. R.: Trophic interactions in the methanogenic microbial community of low-temperature
terrestrial ecosystems, FEMS Microbiol Ecol, 53, 3-13, <https://doi.org/10.1016/j.femsec.2004.12.009>, 2005.
- 788 Laine, J., Minkinen, K., and Trettin, C.: Direct Human Impacts on the Peatland Carbon Sink, in: Carbon Cycling
in Northern Peatlands, Geoph Mono, 71-78, <https://doi.org/10.1029/2008gm000808>, 2013.
- 790 Landesamt für Bergbau, Energie und Geologie (LBEG): RV: 4.25 Richtlinien über das Verfüllen auflässiger
Bohrungen, 1998.
- 792 Le Mer, J. and Roger, P.: Production, oxidation, emission and consumption of methane by soils: A review, Eur J
Soil Biol, 37, 25-50, [https://doi.org/10.1016/s1164-5563\(01\)01067-6](https://doi.org/10.1016/s1164-5563(01)01067-6), 2001.
- 794 Liu, Y. and Whitman, W. B.: Metabolic, phylogenetic, and ecological diversity of the methanogenic archaea,
Ann N Y Acad Sci, 1125, 171-189, <https://doi.org/10.1196/annals.1419.019>, 2008.
- 796 Lubbers, I. M., van Groenigen, K. J., Fonte, S. J., Six, J., Brussaard, L., and van Groenigen, J. W.: Greenhouse-
gas emissions from soils increased by earthworms, Nat Clim Change, 3, 187-194,
798 <https://doi.org/10.1038/nclimate1692>, 2013.
- 800 Martin, M.: Cutadapt removes adapter sequences from high-throughput sequencing reads, EMBnet J, 17,
<https://doi.org/10.14806/ej.17.1.200>, 2011.
- 802 Milkov, A. V. and Etiope, G.: Revised genetic diagrams for natural gases based on a global dataset of >20,000
samples, Org Geochem, 125, 109-120, <https://doi.org/10.1016/j.orggeochem.2018.09.002>, 2018.
- 804 Moore, T. R. and Dalva, M.: Methane and carbon dioxide exchange potentials of peat soils in aerobic and
anaerobic laboratory incubations, Soil Biol Biochem, 29, 1157-1164, [https://doi.org/10.1016/s0038-0717\(97\)00037-0](https://doi.org/10.1016/s0038-0717(97)00037-0), 1997.
- 806 Nakamura, F. M.: Microcosms and the role of active microbiota on methane cycle in soils under Forest and
Pasture of Eastern Amazon, Centro de Energia Nuclear na Agricultura, Universidade de São Paulo,
808 Piracicaba, 117 pp., <https://doi.org/10.11606/T.64.2019.tde-14072021-141002>, 2019.
- 810 Pfadenhauer, J. and Klötzli, F.: Restoration experiments in middle European wet terrestrial ecosystems: an
overview, Vegetatio, 126, 101-115, <https://doi.org/10.1007/bf00047765>, 1996.



- 812 Raimi, D., Krupnick, A. J., Shah, J. S., and Thompson, A.: Decommissioning Orphaned and Abandoned Oil and
Gas Wells: New Estimates and Cost Drivers, *Environ Sci Technol*, 55, 10224-10230,
<https://doi.org/10.1021/acs.est.1c02234>, 2021.
- 814 Rankin, T., Strachan, I. B., and Strack, M.: Carbon dioxide and methane exchange at a post-extraction, unrestored
peatland, *Ecol Eng*, 122, 241-251, <https://doi.org/10.1016/j.ecoleng.2018.06.021>, 2018.
- 816 Romanak, K., Yang, C., and Darvari, R.: Towards a Method for Leakage Quantification and Remediation
Monitoring in the Near-surface at Terrestrial CO₂ Geologic Storage Sites, *Enrgy Proced*, 114, 3855-3862,
818 <https://doi.org/10.1016/j.egypro.2017.03.1517>, 2017.
- Romanak, K. D., Bennett, P. C., Yang, C., and Hovorka, S. D.: Process-based approach to CO₂ leakage detection
820 by vadose zone gas monitoring at geologic CO₂ storage sites, *Geophys Res Lett*, 39,
<https://doi.org/10.1029/2012gl052426>, 2012.
- 822 Romanak, K. D., Wolaver, B., Yang, C., Sherk, G. W., Dale, J., Dobeck, L. M., and Spangler, L. H.: Process-
based soil gas leakage assessment at the Kerr Farm: Comparison of results to leakage proxies at ZERT and
824 Mt. Etna, *Int J Greenh Gas Con*, 30, 42-57, <https://doi.org/10.1016/j.ijggc.2014.08.008>, 2014.
- Saunio, M., Stavert, A. R., Poulter, B., Bousquet, P., Canadell, J. G., Jackson, R. B., Raymond, P. A.,
826 Dlugokencky, E. J., Houweling, S., Patra, P. K., Ciais, P., Arora, V. K., Bastviken, D., Bergamaschi, P.,
Blake, D. R., Brailsford, G., Bruhwiler, L., Carlson, K. M., Carrol, M., Castaldi, S., Chandra, N., Crevoisier,
828 C., Crill, P. M., Covey, K., Curry, C. L., Etiope, G., Frankenberg, C., Gedney, N., Heggin, M. I., Höglund-
Isaksson, L., Hugelius, G., Ishizawa, M., Ito, A., Janssens-Maenhout, G., Jensen, K. M., Joos, F., Kleinen, T.,
830 Krummel, P. B., Langenfelds, R. L., Laruelle, G. G., Liu, L., Machida, T., Maksyutov, S., McDonald, K. C.,
McNorton, J., Miller, P. A., Melton, J. R., Morino, I., Müller, J., Murguia-Flores, F., Naik, V., Niwa, Y.,
832 Noce, S., O'Doherty, S., Parker, R. J., Peng, C., Peng, S., Peters, G. P., Prigent, C., Prinn, R., Ramonet, M.,
Regnier, P., Riley, W. J., Rosentretter, J. A., Segers, A., Simpson, I. J., Shi, H., Smith, S. J., Steele, L. P.,
834 Thornton, B. F., Tian, H., Tohjima, Y., Tubiello, F. N., Tsuruta, A., Viovy, N., Voulgarakis, A., Weber, T. S.,
van Weele, M., van der Werf, G. R., Weiss, R. F., Worthy, D., Wunch, D., Yin, Y., Yoshida, Y., Zhang, W.,
836 Zhang, Z., Zhao, Y., Zheng, B., Zhu, Q., Zhu, Q., and Zhuang, Q.: The Global Methane Budget 2000–2017,
Earth Syst Sci Data, 12, 1561-1623, <https://doi.org/10.5194/essd-12-1561-2020>, 2020.
- 838 Savage, K., Phillips, R., and Davidson, E.: High temporal frequency measurements of greenhouse gas emissions
from soils, *Biogeosciences*, 11, 2709-2720, <https://doi.org/10.5194/bg-11-2709-2014>, 2014.
- 840 Schloss, P. D., Westcott, S. L., Ryabin, T., Hall, J. R., Hartmann, M., Hollister, E. B., Lesniewski, R. A., Oakley,
B. B., Parks, D. H., Robinson, C. J., Sahl, J. W., Stres, B., Thallinger, G. G., Van Horn, D. J., and Weber, C.
842 F.: Introducing mothur: open-source, platform-independent, community-supported software for describing and
comparing microbial communities, *Appl Environ Microbiol*, 75, 7537-7541,
844 <https://doi.org/10.1128/AEM.01541-09>, 2009.
- Schoell, M.: The hydrogen and carbon isotopic composition of methane from natural gases of various origins,
846 *Geochim Cosmochim Acta*, 44, 649-661, [https://doi.org/10.1016/0016-7037\(80\)90155-6](https://doi.org/10.1016/0016-7037(80)90155-6), 1980.
- Schwen, A., Jeitler, E., and Böttcher, J.: Spatial and temporal variability of soil gas diffusivity, its scaling and
848 relevance for soil respiration under different tillage, *Geoderma*, 259-260, 323-336,
<https://doi.org/10.1016/j.geoderma.2015.04.020>, 2015.
- 850 Sechman, H.: Detailed analysis of gaseous components in soil gases around petroleum wells - An effective tool
for evaluation of their integrity, *App Geochem*, 142, <https://doi.org/10.1016/j.apgeochem.2022.105346>, 2022.
- 852 Sikora, A., Detman, A., Chojnacka, A., and Blaszczyk, M. K.: Anaerobic Digestion: I. A Common Process
Ensuring Energy Flow and the Circulation of Matter in Ecosystems. II. A Tool for the Production of Gaseous
854 Biofuels, in: *Fermentation Processes*, <https://doi.org/10.5772/64645>, 2017.



- 856 Strack, M., Keith, A. M., and Xu, B.: Growing season carbon dioxide and methane exchange at a restored
peatland on the Western Boreal Plain, *Ecol Eng*, 64, 231-239, <https://doi.org/10.1016/j.ecoleng.2013.12.013>,
2014.
- 858 Strack, M., Cagampan, J., Fard, G. H., Keith, A. M., Nugent, K., Rankin, T., Robinson, C., Strachan, I. B.,
Waddington, J. M., and Xu, B.: Controls on plot-scale growing season CO₂ and CH₄ fluxes in restored
860 peatlands: Do they differ from unrestored and natural sites?, *Mires Peat*, 17, 1-18,
<https://doi.org/10.19189/MaP.2015.OMB.216>, 2016.
- 862 Sundh, I., Nilsson, M., Granberg, G., and Svensson, B. H.: Depth distribution of microbial production and
oxidation of methane in northern boreal peatlands, *Microb Ecol*, 27, 253-265,
864 <https://doi.org/10.1007/BF00182409>, 1994.
- Sundh, I., Nilsson, M., Mikkela, C., Granberg, G., and Svensson, B. H.: Fluxes of Methane and Carbon Dioxide
866 on peat-mining Areas in Sweden, *AMBIO*, 29, 499-503, <https://doi.org/10.1579/0044-7447-29.8.499>, 2000.
- Takai, K. and Horikoshi, K.: Rapid detection and quantification of members of the archaeal community by
868 quantitative PCR using fluorogenic probes, *Appl Environ Microbiol*, 66, 5066-5072,
<https://doi.org/10.1128/AEM.66.11.5066-5072.2000>, 2000.
- 870 Turetsky, M. R., Kotowska, A., Bubier, J., Dise, N. B., Crill, P., Hornibrook, E. R., Minkinen, K., Moore, T. R.,
Myers-Smith, I. H., Nykanen, H., Olefeldt, D., Rinne, J., Saarnio, S., Shurpali, N., Tuittila, E. S., Waddington,
872 J. M., White, J. R., Wickland, K. P., and Wilming, M.: A synthesis of methane emissions from 71 northern,
temperate, and subtropical wetlands, *Glob Chang Biol*, 20, 2183-2197, <https://doi.org/10.1111/gcb.12580>,
874 2014.
- Versantvoort, W., Guerrero-Cruz, S., Speth, D. R., Frank, J., Gambelli, L., Cremers, G., van Alen, T., Jetten, M.
876 S. M., Kartal, B., Op den Camp, H. J. M., and Reimann, J.: Comparative Genomics of *Candidatus*
Methylomirabilis Species and Description of *Ca. Methylomirabilis Lanthanidiphila*, *Front Microbiol*, 9, 1672,
878 <https://doi.org/10.3389/fmicb.2018.01672>, 2018.
- Webster, G., Newberry, C. J., Fry, J. C., and Weightman, A. J.: Assessment of bacterial community structure in
880 the deep sub-seafloor biosphere by 16S rDNA-based techniques: a cautionary tale, *J Microbiol Methods*, 55,
155-164, [https://doi.org/10.1016/s0167-7012\(03\)00140-4](https://doi.org/10.1016/s0167-7012(03)00140-4), 2003.
- 882 Welpelo, C., Dubbert, M., Tiemeyer, B., Voigt, C., and Piayda, A.: Effects of birch encroachment, water table
and vegetation on methane emissions from peatland microforms in a rewetted bog, *Sci Rep*, 14, 2533,
884 <https://doi.org/10.1038/s41598-024-52349-0>, 2024.
- Whiticar, M. J.: The Biogeochemical Methane Cycle, in: *Hydrocarbons, Oils and Lipids: Diversity, Origin,*
886 *Chemistry and Fate*, 1-78, https://doi.org/10.1007/978-3-319-54529-5_5-1, 2020
- Whiticar, M. J.: Carbon and hydrogen isotope systematics of bacterial formation and oxidation of methane, *Chem*
888 *Geol*, 161, 291-314, [https://doi.org/10.1016/s0009-2541\(99\)00092-3](https://doi.org/10.1016/s0009-2541(99)00092-3), 1999.
- Wilson, D., Farrell, C. A., Fallon, D., Moser, G., Muller, C., and Renou-Wilson, F.: Multiyear greenhouse gas
890 balances at a rewetted temperate peatland, *Glob Chang Biol*, 22, 4080-4095,
<https://doi.org/10.1111/gcb.13325>, 2016.
- 892 Wittnebel, M., Frank, S., and Tiemeyer, B.: Aktualisierte Kulisse organischer Böden in Deutschland. [dataset],
<https://doi.org/10.3220/DATA20230510130443-0>, 2023.
- 894 Yang, S., Wen, X., and Liebner, S.: *pmoA* gene reference database (fasta-formatted sequences and taxonomy)
[dataset], <https://doi.org/10.5880/GFZ.5.3.2016.001>, 2016.